

A
Dissertation Report on
**Design and Development of a Rotary Torque
Sensor**

Submitted
in partial fulfilment of the requirements for the degree of
Master of Technology
in
Mechanical Design

by
Mr. Powar Suraj Shankar
(Roll No. 1921005)

Sponsored by
Trilon Technology, Pune

Under the Supervision of
Dr. M. B. Mandale



Department of Mechanical Engineering
K.E. Society's
Rajarambapu Institute of Technology, Rajaramnagar
(An Autonomous Institute, Affiliated to Shivaji University, Kolhapur)
2020-2021

K.E. Society's
Rajarambapu Institute of Technology, Rajaramnagar
(An Autonomous Institute, Affiliated to Shivaji University, Kolhapur)

CERTIFICATE

This is to certify that, Mr. Suraj Shankar Powar (Roll No-1921005) has successfully completed the dissertation work and submitted dissertation report on (“Design and Development of a Rotary Torque Sensor”) for the partial fulfillment of the requirement for the degree of Master of Technology in Mechanical Design from the Department of Mechanical Engineering., as per the rules and regulations of Rajarambapu Institute of Technology, Rajaramnagar, Dist: Sangli.

Date:

Place: RIT, Rajaramnagar

Dr. M. B. Mandale

Mr A. S. Koli

Name and Sign of Supervisor

Name and Sign of Industrial Supervisor

Name

Dr. S. S. Gawade

Name and Sign of External Examiner

Name and Sign of Head of Program

Dr. S. K. Patil

Dr. S. S. Gawade

Name and Sign of Head of Department

Name and Sign of PG Convener

Here join Company Project Completion certificate on Letterhead of company along with competent authority sign, stamp and outward number.

DECLARATION

I declare that this report reflects my thoughts about the subject in my own words. I have sufficiently cited and referenced the original sources, referred or considered in this work. I have not misrepresented or fabricated or falsified any idea/data/fact/source in this my submission. I understand that any violation of the above will be cause for disciplinary action by the Institute.

Place: RIT, Rajaramnagar

Name of Student: Suraj Shankar Powar

Date:

Roll No: 1921005

ACKNOWLEDGEMENTS

I must mention several individuals and organizations that were of enormous help in the development of this work. The Company Trilon Technology, Pune and My Industrial supervisor Mr. A. S. Koli and their colleagues Mr. Pankaj Kolhe and Mr. Ketan Dhage for continuous support and guidance. Also Professor M. B. Mandale my supervisor, philosopher and personality with a midas touch encouraged me to carry this work. His continuous invaluable knowledgeable guidance throughout the course of this study helped me to complete the work up to this stage and hope will continue in further research.

I also very thankful to HoP, HoD for their valuable suggestions, critical examination of work during the progress, I am indebted to them.

I am very grateful to Akshay and Vipul for his positive cooperation and immense kindly help during the period of work with him.

In addition, very energetic and competitive atmosphere of the Mechanical Engineering Department had much to do with this work. I acknowledge with thanks to faculty, teaching and non-teaching staff of the department, Central library and Colleagues.

I sincerely thank to Dr. Mrs. S. S. Kulkarni Director of RIT, for supporting me to do this work and I am very much obliged to her.

Last but not the least; Mr. Shankar Powar, my father and Mrs. Gitanjali Powar, my mother, constantly supported me for this work in all aspects

Place: RIT, Rajaramnagar

Name of Student: Suraj Powar

Date:

Roll No: 1921005

ABSTRACT

Rotary Torque sensor, which uses strain gauges as their measuring element to respond against the stresses in torsion bars caused due to applied torque are widely used to measure a wide range of torques in numerous applications. Moreover torque measurement is a very complicated process so it requires special solution for each case. In this dissertation a new torque determination process by using a new shape of strain gauge is used to design and develop a rotary shaft to shaft torque sensor for use of torque value determination work. During the design of strain gauge based rotary torque sensor two strain gauges are considered to make a bridge circuit. Several torque sensors, which are currently being used, are studied and then this new rotary torque sensor is designed with the help of finite element analysis. The finite element analysis is performed on shaft by considering the properties of SS304 as a material of shaft. The design and analysis work is done by considering the boundary conditions for a 100 NM torque capacity and FOS as 1.5. Then the core part that is the shaft is manufactured and actual experimental testing is completed by gauge pasting and values are obtained through data acquisition system. The results of mathematical calculations, FEA analysis results, and experimental results are compared.

Keywords: Torque Sensor, Strain gauge, FEA analysis.

Contents

<i>CERTIFICATE</i>	ii
<i>SPONSORSHIP CERTIFICATE</i>	iii
<i>DECLARATION</i>	iv
<i>ACKNOWLEDGEMENTS</i>	v
<i>ABSTRACT</i>	vi
<i>CONTENT</i>	vii
<i>LIST OF FIGURES</i>	xi
<i>LIST OF TABLES</i>	xii
<i>NOMENCLATURE</i>	xiii
<i>ABBREVIATIONS</i>	xiv
1 Introduction	1
1.1 Introduction	1
1.2 Principle of torque sensor	2
1.3 Definition of torque	4
1.4 Strain gauge transducers	5
1.4.1 Structure of strain gauges	5
1.4.2 Principle of strain gauges	6
1.4.3 What is Wheatstone bridge?	7
1.4.4 Bridge Structures	8
1.5 Temperature Compensation	10
1.5.1 Active dummy method	11
1.5.2 Self temperature compensation method	11
2 Literature Review	13
2.1 Introduction	13
2.2 Classification of Literature Review	13

2.2.1	Electrical domain	13
2.2.2	Electronics / Electromagnetic phenomena	18
2.2.3	Optical domain	19
2.3	Literature Outcome	20
2.4	Problem statement	22
2.5	Objectives of present work	22
3	Design and Specifications	24
3.1	Design Fundamentals	24
3.2	Design of shaft	25
3.3	Finite Element Analysis of Shaft	25
3.3.1	Oversized Shaft Condition	27
3.3.2	Undersized Shaft Condition	28
3.3.3	Optimum Shaft Design	28
3.4	FEA for optimum design shaft	29
3.4.1	Ansys Strain Results	29
3.4.2	Ansys Stress Results	29
3.4.3	Ansys Plastic Strain Results	30
3.5	Signal Transmission System	31
3.6	Bearing Specifications	31
3.7	Sensor Housing Design and Proposed Assembly Setup	32
4	Experimental Work and Calibration	37
4.1	Strain gauging Selection	37
4.1.1	Strain Gauge Circuit Connections	38
4.1.2	Manufacturing of Sensor Shaft	38
4.1.3	Strain Gauge Pasting	39
4.2	Experimentation on Setup	41
4.2.1	Torque Setup Specifications	41
4.2.2	Experimentation	42
4.2.3	Data Acquisition System Specifications	44
4.3	Cost of experimental testing	45
5	Results and Discussion	46
5.1	Introduction	46

5.2	Material Properties and Formulas considered for Calculation	46
5.3	Analytical Results	47
5.4	Finite Element Analysis Results	48
5.5	Experimental results	48
5.6	Results Graphs	49
5.7	Discussion on Results	50
6	Conclusion	51
	<i>LIST OF PUBLICATIONS ON PRESENT WORK</i>	53
	<i>REFERENCES</i>	54

List of Figures

1.1	Principle of a typical rotary torque sensor	3
1.2	Strain due to twisting of shaft	4
1.3	definition of torque	5
1.4	Structure of strain gauge	6
1.5	Bridge structure by combining four resistors	7
1.6	Output of one gauge system	8
1.7	Output of four gauge system	9
1.8	Output of two gauge system	10
1.9	Active dummy method	11
1.10	Self compensation gauge	12
3.1	Torque sensor dimensions	24
3.2	Design of shaft	25
3.3	Fixed Support Boundary conditions used during FEA	26
3.4	Cylindrical Support Boundary conditions used during FEA	26
3.5	Applied Moment Boundary conditions used during FEA	27
3.6	Oversized shaft design condition	27
3.7	Undersized Shaft Condition	28
3.8	Optimum Shaft design condition	28
3.9	Ansys strain results for optimum shaft design	29
3.10	Ansys stress results for optimum shaft design	30
3.11	Ansys plastic strain results for optimum shaft design	30
3.12	Bearing Specifications	31
3.13	Sensor Housing dimensions	33
3.14	Sensor Housing Design	33
3.15	Casing cover plate with connector dimensions	34

3.16	design of Cover plate with connector	34
3.17	Assembly view of sensor	35
3.18	Exploded view of sensor	35
3.19	BOM and the quantity of components required for the sensor to be a end product	36
4.1	Strain gauge details	37
4.2	Strain Gauge Circuit	38
4.3	Manufactured Sensor Shaft	39
4.4	Surface Cleaning and Gauge location marking	40
4.5	Strain gauge pasting and Soldering	40
4.6	Gauge wire soldering and Gauge area covering	41
4.7	Experimental Setup	42
4.8	Experimentation on Shaft	43
4.9	Data Acquisition Setup	44
4.10	e-DAQ Processor and signal conditioning layers	45
4.11	Cost of experimental testing	45
5.1	Formulas used for Calculation	47
5.2	Result Comparison Graph	49
6.1	Proposed design of Slip ring and Brushes	52

List of Tables

2.1	Comparison study of different principle of torque sensors	21
2.2	Torque sensor manufacturers and its prices	22
3.1	Dimensions of Rotary torque sensors	24
5.1	Material Properties	46
5.2	Reference values used for calculation	47
5.3	Analytical calculation results	48
5.4	FEA results	48
5.5	Experimental Results	49

NOMENCLATURE

γ	Shear Strain
μ	Poissons Ratio
τ	Shear Stress (Mpa)
Θ	Angle of Twist (degree)
D	Diameter of Shaft (Meter)
E	Modulus of Elasticity (N/M ²)
e	Bridge Output Voltage (mV)
Ev	Excitation Voltage (Volts)
G	Modulus of Rigidity (N/M ²)
J	Polar Moment of Inertia (M ⁴)
K	Gauge Factor
L	Length of Shaft(Meter)
R	Radius of Shaft (Meter)
T	Torque (N.m)

ABBREVIATIONS

DAQ	Data Acquisition
NIEJ	National Instrument and Engineering Jaipur
CNC	Computer Numerical Control
FEA	Finite Element Analysis
SRB	Slip Ring and Brushes
LVDT	Linear Variable Differential Transformers

Chapter 1

Introduction

1.1 Introduction

In simple terms, a torque measurement sensor can be defined as a sensor that converts the torque measurement value (reaction, dynamic or rotation) into an additional measurement variable, where it is converted into an electrical signal that can be measured, converted, and normalized. Torque measurement is generally divided into static torque measurement and dynamic torque measurement. In a static measurement system, the measured torque is the torque of rotating a stationary object. In case of dynamic measurement system, the body is revolved or rotated by the applied torque. Torque measurement in static structures is easier than in dynamic structures. This is because dynamics has some difficulties in transmitting measurement signals between static and rotating parts. The amount of torque can be determined by measuring force and displacement, rotation angle, shear stress or strain.

Torque converters are commonly used as engine test/test tools, torque measurement tools, turbines and generators to measure torque. The rotating shaft-to-axis torque sensor can also be used for feedback control, monitoring torque and analyzing the efficiency of the test bench, as well as measuring the torque on the rotating shaft. Torque sensor is a device that can also be used to measure torque on rotating systems such as rotors, hammer mills, and gears. When trying to optimize power consumption, torque measurement plays an important role in controlling the power of a mechanical system. In such a system, the rotating shaft torque sensor is very important. On the other hand, in the automation application field

of today's mechanical industry, with the establishment of more and more mechanical product capabilities, the demand for torque measurement is also increasing. Torque measurement is essential for improving machine efficiency in the control part of the power transmission system. Therefore, accurate, reliable and inexpensive torque detection and measurement are required. Therefore, a new torque sensor concept based on a highly reliable measurement principle will be designed and developed. The basic idea is to convert the shaft rotation under the torque load into the signal input of the sensor element, and then display the measured value by the measuring device. Therefore, in most cases where a torque sensor is used, it has a dynamic measurement arrangement formed by a shaft-to-shaft connection. For real-world use in mechanical systems, the torque sensor need to be effortlessly mounted on the shaft, and the shaft torque must be recorded with high precision and accuracy.

This work focuses on strain gauge-based torque-torque sensors, aiming to improve its mechanical parameter optimization and scalability. The most common commercial single-axis torque sensor geometry is a solid round shaft. The solid shaft has structural advantages, especially in high load applications; it provides high bending strength and simple application of strain gauges. The goal is to develop a simple geometric structure that allows strain gauges to be easily attached to the shaft surface to detect the strain due to the applied torque. For design purposes, various designs of available torque sensors were checked, and the number of studies reported was also considered. In the design, an important factor that also compromises the performance of the torque sensor is related to the shaft that connects the strain gauge to the sensor, because it affects the shape and achievable performance.

The main aim of the work is to propose an enhanced strain gauge based torque transducer for measuring dynamic loading on a rotary shaft.

1.2 Principle of torque sensor

In terms of design, the torque device consists of a metal body (rotating shaft) to which the strain gauges are connected. The sensor shaft is usually made of aluminum or stainless steel, which provides the sensor with two basic characteristics: (1) strong to withstand high torque; (2) elastic to minimize deformation when the

torque is released and restore its original shape. When a torque is applied, the metal body as the rotating shaft is like a "spring" and is easily deformed. If it is not overloaded, it will return to its original shape.

In a rotary torque sensor, the strain gauge is connected to the rotating shaft, and when a torque is applied, the rotating shaft rotates slightly. Shaft rotation will generate stress in the strain, and the strain gauge will also change its shape, thereby changing its resistance, thereby generating a difference in voltage change through the Wheatstone bridge circuit. Therefore, the voltage change is proportional to the torque applied to the converter and can be calculated, calibrated and measured by the voltage output of the torque sensor circuit. The rotating torque sensor is designed to measure the torque of a rotating shaft. Therefore, what is important is the means to transmit the force to the strain gauge bridge and to receive the signal from the torque gauge or shaft. This can be done through slip rings, wireless telemetry or resolvers. The sensor output is a function of force and displacement, usually expressed in Newton meters (Nm)

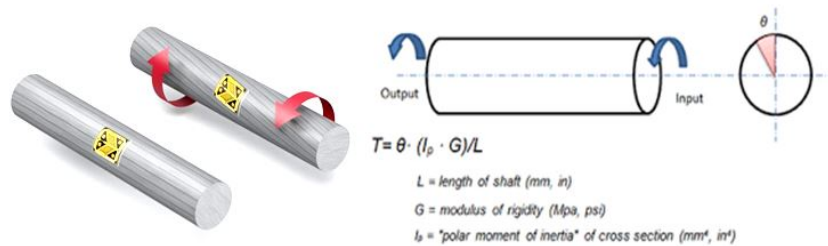


Figure 1.1: Principle of a typical rotary torque sensor

Relation between the strain due to torsion:-

Torsion means the twisting of a body caused by moment acting around the objects longitudinal axis. So when a torque is applied to a solid circular bar (shaft) it causes it to deform by twisting. As A Result of it generates stresses and strains in the bar. The general torsion equation is $\frac{T}{J} = \frac{\tau}{R} = \frac{G\theta}{L}$ In case of the torque sensors where the strain gauges are used, the torque is calculated by means of capturing the strain due to the deformation by twisting of shaft after application of torque.

So to obtain the strain value consider a small rectangular element on surface of shaft as shown in fig 1.2 (b). The element CDEF as shown in figure is rectangular before the torque application, once the torque is applied it get distorted. Now

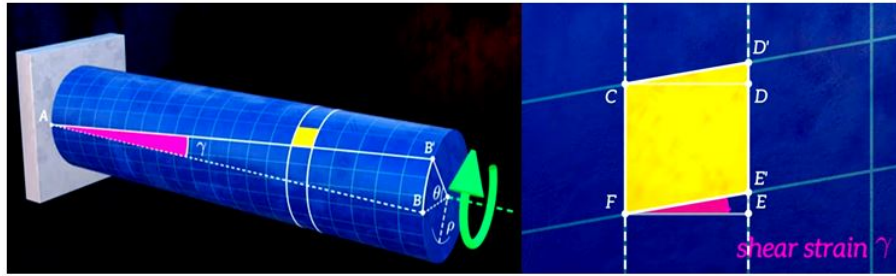


Figure 1.2: Strain due to twisting of shaft

due the small deformation the angle of small elements will no longer remain at 90 degree and become CD'E'F' this gives rise to a shear strain which corresponds to an angle E'FE as shown in figure. This shear strain can be obtained by considering the geometry of bar in twist. By using trigonometry to derive an equation for γ (shear strain) By trigonometry for small angles, $\gamma = \tan\gamma$.

$$\tan\gamma = \frac{BB'}{AB} = \frac{BB'}{L} = \frac{r\theta}{L}$$

So the shear strain is equal to the radius of bar (r) multiplied by angle of twist (θ) divided by length of bar (L). This equation is only applicable for shear strain on the surface of the bar. So, it is known that shear strain rise linearly with the distance from the center of the cross section.

So if ρ is defined as the radial distance from the center of the cross section and replaced at place of r we can get equation to calculate shear strain due to torsion at any point within the bar,

$$\tan\gamma = \frac{\rho\theta}{L}$$

So, experimentally this equation is used by means of strain gauges to actually measure the strain. Thereafter output of strain gauge is calibrated in terms of the torque value.

1.3 Definition of torque

Torque is a very vital physical factor, which plays an important role in determining the quality of goods. With reference to Figure 1, torque can be approximately defined as a measure of the force that causes object C to rotate.

When subjected to force F , the object rotates around an axis called pivot point O . The distance r from the fulcrum to the point of force application is called the lever arm. Please note that r is also a vector, which points from the axis of rotation to the point of force application. A formula can be used to calculate the amount of torque. (1) The unit of torque is Nm, which is the torque formed by 1N force acting on a point within 1m of the fulcrum radius.

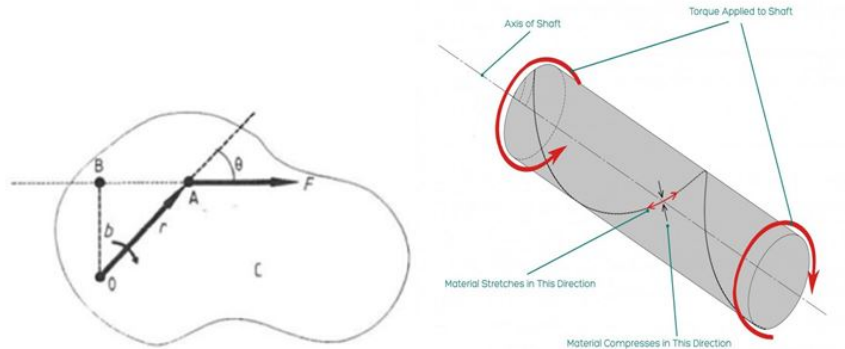


Figure 1.3: definition of torque

This definition applies to static torque measurement and dynamic torque measurement. More generally, the torque can be defined as;

$$T = \vec{r} \times \vec{F} \quad (1.1)$$

In the single dimensional case

$$T = r \cdot F \cdot \sin \theta \quad (1.2)$$

Where, θ is the angle among the position vector, r and the force vector, F . In the case of a shaft revolving with angular velocity and power P , torque can be also calculated from:

$$T = \frac{P}{\omega} \quad (1.3)$$

1.4 Strain gauge transducers

1.4.1 Structure of strain gauges

There are numerous kinds of strain gauges. Between them a common strain gauge has a structure such that a grid shaped sensing part of thin metallic resistive foil

(3 – 6 μm) is put on the base of a thin plastic film (15 – 16 μm) and is covered with a thin film

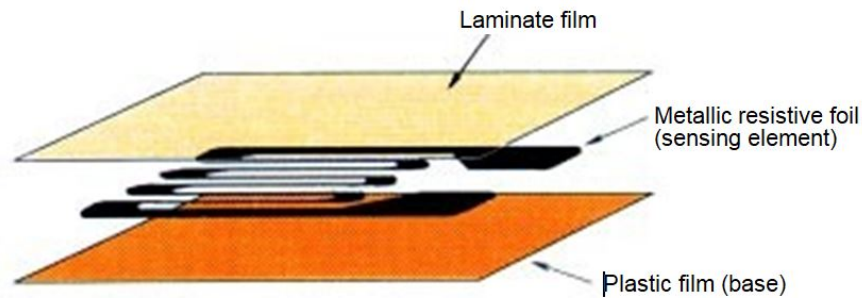


Figure 1.4: Structure of strain gauge

1.4.2 Principle of strain gauges

The strain gauge is connected with the measuring unit, so that the measuring element (metal resistance foil) expands or contracts according to the expansion of the measured object. The resistance changes due to expansion or contraction. Strain gauges apply this principle to strain measurement by changes in resistance. Normally, the sensor element of the strain gauge is made of copper-nickel blend foil. The resistance change of the alloy foil is proportional to the elongation and has a certain constant. Let's express the principle as follows:

$$\frac{\Delta R}{R} = K\varepsilon \quad (1.4)$$

Where, R: Original resistance of strain gauge, Ω (ohm)

ΔR : Elongation or contraction initiated resistance change, Ω (ohm)

K: Proportionate constant (called gauge factor)

ε : Strain

The K factor K varies depending on the metal material. The coefficient of measurement for the copper-nickel mixture (Advance) is approximately 2. Therefore, a strain gauge using this alloy as a measuring element can convert mechanical strain into an equivalent resistance variation. However, since the load is an invisible phenomenon, the resistance change caused by the load is small.

In fact, it is very challenging to accurately measure small changes in resistance, which cannot be measured by traditional ohmmeters. Therefore, small changes

in resistance are measured by a devoted strain amplifier using a circuit called a Wheatstone bridge.

1.4.3 What is Wheatstone bridge?

The Wheatstone bridge is an electric circuit appropriate for finding of minute resistance variations. It is hence used to measure resistance changes of a strain gauge. Suppose the bridge is constructed by merging four resistors as shown in figure. If $R_1=R_2=R_3=R_4$, or $R_1 \cdot R_3=R_2 \cdot R_4$

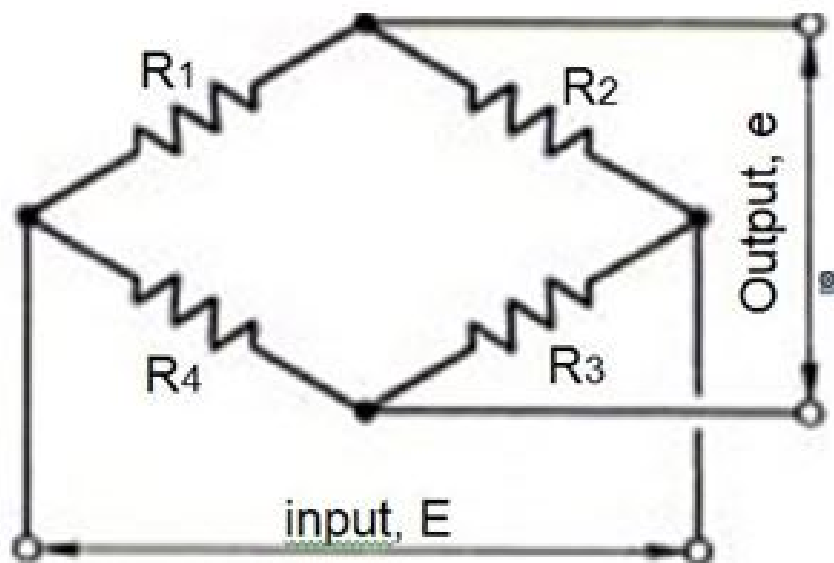


Figure 1.5: Bridge structure by combining four resistors

Then whatsoever voltage is applied to the input, the output, e , is zero. Such a bridge position is called “balanced” When the bridge loses the stability; it outputs a voltage resultant to the resistance variation. As shown in figure a strain gauge is linked in place of R_1 in the circuit. When the gauge bears strain and induces a resistance variation, ΔR , the bridge outputs a equivalent voltage, e .

$$e = \frac{1}{4} \cdot \frac{\Delta R}{R} \cdot E \quad (1.5)$$

That is,

$$e = \frac{1}{4} \cdot \frac{\Delta R}{R} \cdot \varepsilon \cdot E \quad (1.6)$$

Meanwhile values other than ε are well-known values, strain, ε , can be determined by measuring the bridge output voltage.

1.4.4 Bridge Structures

The most commonly found structures are 1- gauge system, 2- gauge system and 4- gauge system.

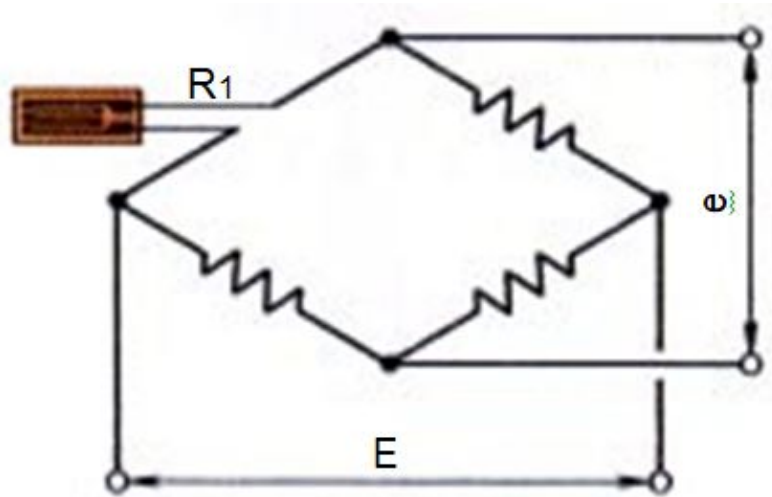


Figure 1.6: Output of one gauge system

1-Gauge system

In 1 gauge system only one gauge is used. In the 1 gauge system undergoes resistance change at R1 one side only, shown in figure 1.4 Output voltage of 1-gauge system:-

$$e = \frac{1}{4} \cdot \frac{\Delta R1}{R1} \cdot E \quad (1.7)$$

Or

$$e = \frac{1}{4} \cdot K \cdot \epsilon \cdot E \quad (1.8)$$

In almost all cases, general strain measurement is performed using the 1 gauge system.

4-Gauge system

In case of 4 gauges system it has four gauges connected shown in figure 1.5 one each to all four edges of the bridge. Although this system is hardly used for strain measurement, it is often applied to strain gauge transducers. Output voltage of 4-gauge system:- When the gauges at the four sides have their resistance altered to $R1 + \Delta R1$, $R2 + \Delta R2$, $R3 + \Delta R3$ and $R4 + \Delta R4$ correspondingly the bridge output

voltage, e , is;

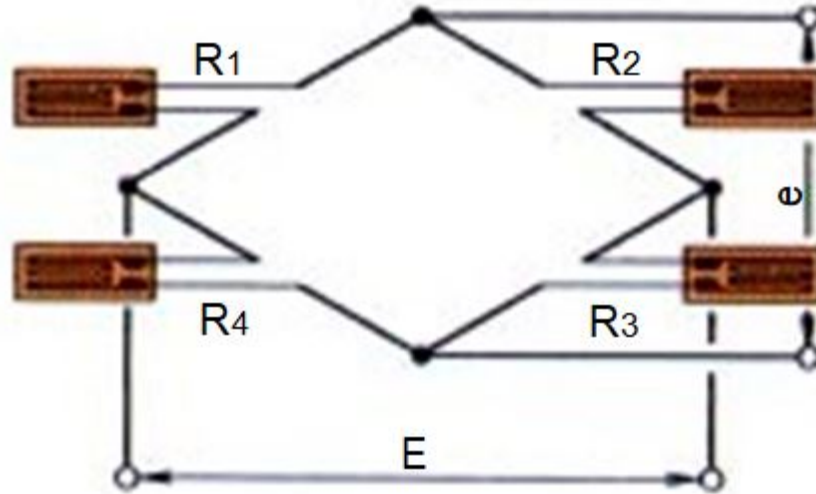


Figure 1.7: Output of four gauge system

$$e = \frac{1}{4} \cdot \left(\frac{\Delta R1}{R1} - \frac{\Delta R2}{R2} + \frac{\Delta R3}{R3} - \frac{\Delta R4}{R4} \right) \cdot E \quad (1.9)$$

If the gauges at the four sides are equivalent in specifications as well as the gauge factor, K , and obtain strains, $\varepsilon1$, $\varepsilon2$, $\varepsilon3$ and $\varepsilon4$, respectively, the equation above will be:

$$e = \frac{1}{4} \cdot K \cdot (\varepsilon1 - \varepsilon2 + \varepsilon3 - \varepsilon4) \cdot E \quad (1.10)$$

2-Gauge system

With the 2-gauge system, gauges are linked to the bridge in either of two ways as shown in figure 1.6. Output voltage of two gauge system:- Two sides amongst the four initiated resistance variation. Thus, the gauge system in the case of Fig (a) delivers following output voltage.

$$e = \frac{1}{4} \cdot \left(\frac{\Delta R1}{R1} - \frac{\Delta R2}{R2} \right) \cdot E \quad (1.11)$$

Or

$$e = \frac{1}{4} \cdot K \cdot (\varepsilon1 - \varepsilon2) \cdot E \quad (1.12)$$

In case of fig (b)

$$e = \frac{1}{4} \cdot \left(\frac{\Delta R1}{R1} + \frac{\Delta R3}{R3} \right) \cdot E \quad (1.13)$$

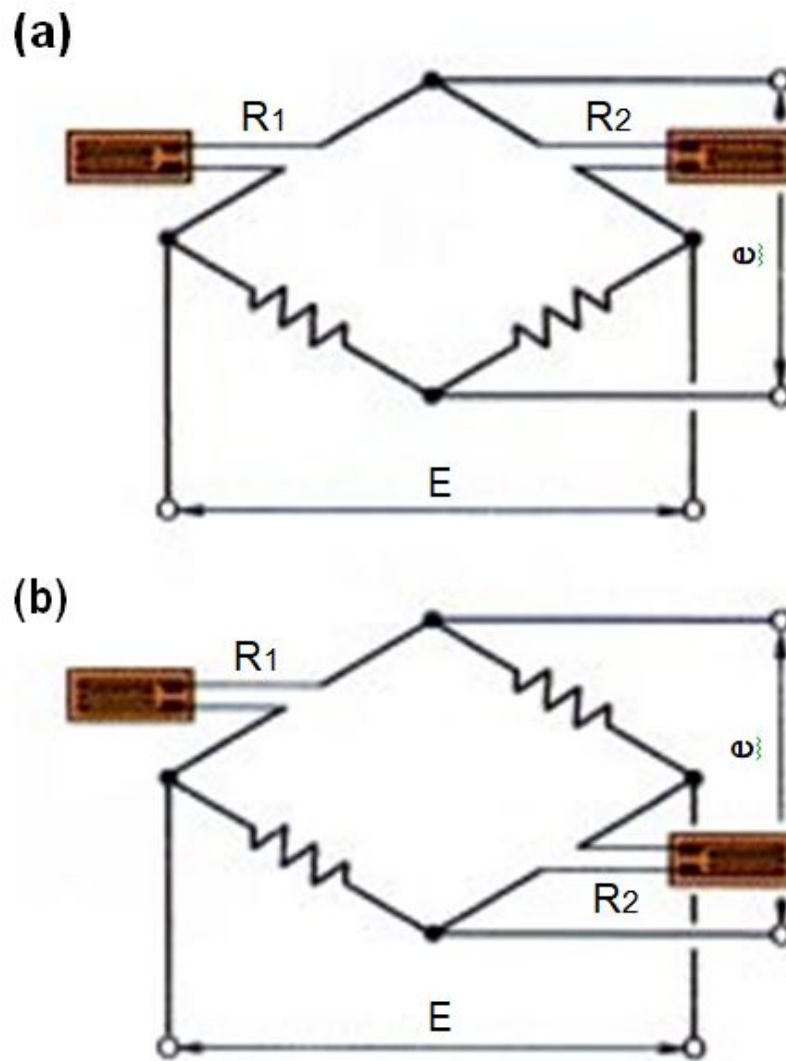


Figure 1.8: Output of two gauge system

Or

$$e = \frac{1}{4} \cdot K \cdot (\epsilon_1 + \epsilon_3) \cdot E \quad (1.14)$$

1.5 Temperature Compensation

One of the difficulties of strain measurement is thermal influence. Except for force, temperature changes make the measuring body lengthen or shorten, which has a certain linear expansion coefficient. Therefore, the strain gauge connected to the object carries thermally induced apparent strain. Temperature compensation resolves this problem. Temperature compensation can be done in two ways,

1.5.1 Active dummy method

Active dummy technology uses a 2-gauge system, in which active dummy A is connected to the measuring prism, and dummy D is connected to a dummy block without a measuring prism load, but under the same temperature conditions as the temperature conditions affecting the measurement object. The virtual block will be made of the same material as the measuring entity.

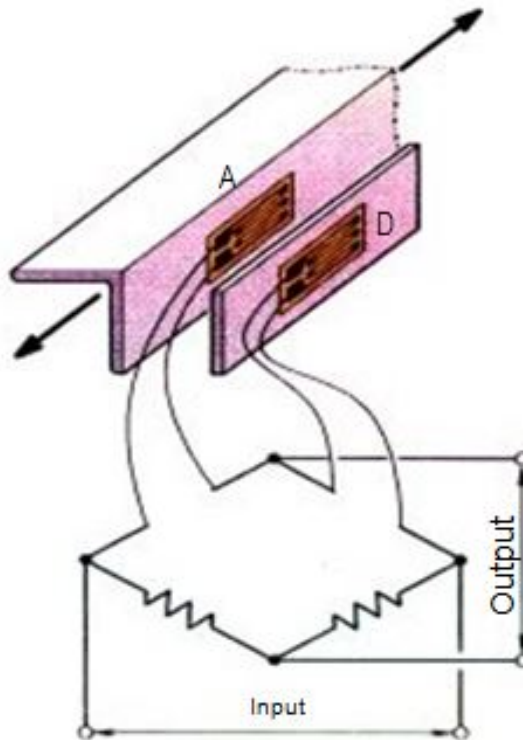


Figure 1.9: Active dummy method

1.5.2 Self temperature compensation method

The temperature coefficient of resistance of the sensor element is controlled by the self-temperature compensation measuring device according to the coefficient of linear expansion of the measuring body. Therefore, if the measuring device matches the measuring object, the measuring device can perform strain measurement without thermal influence. Assume that the linear expansion coefficient of the measuring body is β_s and that of the resistive element of the strain gauge is β_g .

When the strain gauge is bonded to the measuring entity as shown in fig, the

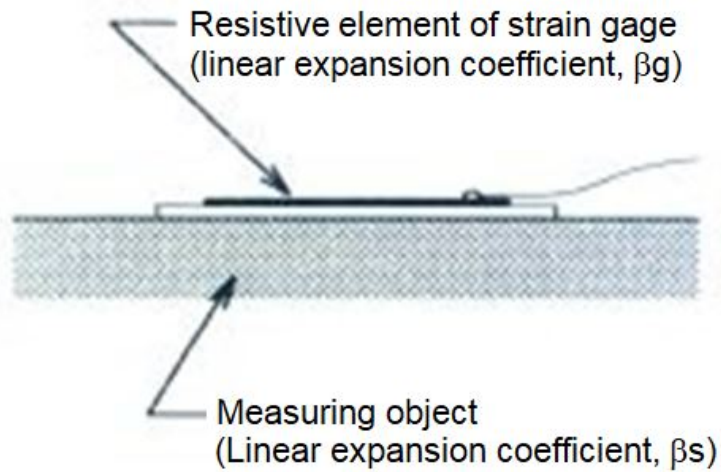


Figure 1.10: Self compensation gauge

strain gauge allows thermally-induced apparent strain/ $^{\circ}\text{C}$, ε_T , as follows:

$$\varepsilon_T = \frac{\alpha}{K_s} + (\beta_g - \beta_s) \quad (1.15)$$

Where, “ α ” is temperature coefficient and “ K_s ” is Gauge factor of strain gauge.

Chapter 2

Literature Review

2.1 Introduction

Torque quantity on rotating shafts leads to a specific design prerequisite. The torque data has to be transmitted from the rotating shaft to the stationary readout environment. The technical resolution is to pick up the torque data on the rotating shaft and transmit it to a static receiver either through electric, magnetic or electromagnetic field. In order to have a detailed and descriptive knowledge of the various principles of different types of strain gauges literature study is more important and helpful.

2.2 Classification of Literature Review

On the basis of measurement of deformation of elastic element the literature review is divided into following parts,

- I. Electrical domain
- II. Electronic / Electromagnetic phenomenon
- III. Optical domain

2.2.1 Electrical domain

[1] Westbrook and Turner, 1994, etc., electrical measurement is basically related to strain gauges, capacitance and piezoelectric sensing. The strain gage process is based on the change in resistance with strain. Once a force is given, the strain will fluctuate the resistance of the meter in proportion to the load. Due to its high

sensitivity, silicon semiconductor strain gauges are often used. The expansion of silicon causes its bulk resistance to change, resulting in a signal that is 75 times stronger than traditional thin-film measurement equipment. In traditional thin-film measurement equipment, resistance fluctuations can only be traced back to the dimensional change of the resistance. Due to the advantages of strain gauges, such as high linearity, about 0.03% 2.5% of the full scale value, and high strength of 13 mV/V, their maximum permissible elongation is close to their breaking limit. In order to ensure the overload protection of the converter, a mechanical stop to limit the deflection of the bending element is indispensable. Very rigid sensors only allow a deflection of tens of thousands of millimeters. It is very difficult to produce the end stop with such a small gap. Strain gauge-based torque/force sensors are exposed to protruding radial and additional force mechanisms. Semiconductor and foil measuring devices require complicated connection procedures by those skilled in the art. Another disadvantage of these sensors is their high sensitivity to electrical noise.

[2] Kovacich 2002 et al. Piezoelectric torque sensors are similar to strain gauges in the process and are based on the phenomenon that crystals are charged under mechanical stress. The high stiffness and strength allow the sensor to be directly integrated into the torsion element. An example of piezoelectric results is the present invention, in which the author uses the change in the resonant frequency of the piezoelectric component as a measure of the load on the torsion element. Very high accurateness (0.03% of full scale) and high signal output are their main benefits. The disadvantages that limit its application are high cost and non-linear output.

[3] Fulmek 2002 and Madni 2004 et al. Many torque converters are designed to measure the relative angle between the two ends of a torsion bar. This principle can be understood using differential capacitive sensors for measuring relative angles. The sensor is non-contact, and the is robust and compact. Two rotatable electrodes are located in the middle of the two sensor plates. The relative angle between the two rotors and the overall position of the rotor blades are calculated by measuring the capacitive connection between different transferring stator seg-

ments and a single receiving electrode. Its disadvantages are high sensitivity to radial displacement and higher cost. The relationship between the capacitance of the capacitor and the dielectric constant of the dielectric material between the capacitor plates is also used. In this development, the perforated metal cage shielding the dielectric rotor is clamped between the capacitor plate rings connected to the opposite sides of the torsion bar. The relative rotation of the perforated conductive plate and the dielectric rotor changes the total differential capacitance of the system.

[4] Hamza Khan, Claudio Semini 2017 and others, strain gauge-based torque sensors are often used to provide high-precision torque measurement in automation. Although it is often necessary to measure the torque/force of the connection in technical research and advancement, when integrating in the limited available space of a small connection table, the bonding and wiring of the strain gauge used as a torque sensor can create complexity. The need for a scalable geometric design to measure joint torque complicates the problem. This document describes a novel design of a single-axis torque sensor based on strain gauges. The sensor is called Squarecut Torque Transducer (SCTS). Its important feature is a high degree of linearity, symmetry and high flexibility in terms of size and measurement range. Scalability. More notably, despite the limited space, SCTS can easily paste and wire strain gauges to the sensor surface. This confirms that SCTS is superior and more linear in terms of symmetry (clockwise and counterclockwise rotation). Finite element modeling (ANSYS) proved these capabilities, and the data obtained through the motion test confirmed this. Studies including changes in size, material, and/or wing width and thickness demonstrate the high performance of SCTS. Finally, it is shown that SCTS can be successfully applied to the hip joint of a miniaturized hydraulically actuated quadruped robot.

[5] Zhang Jiaming, Gong Chen 2015, etc. The rotating shafts of complex heavy industrial equipment such as large generators, rolling mills and wind generators often break due to fatigue cracks caused by torque overload. Online observation of torque is also an important basis for evaluating power system conditions and diagnosing faults. Due to practical problems such as sensor installation, reliability,

and accuracy, the torque test of the high-speed rotating shaft is often unsuccessful, so the observation of the torque of the high-speed rotating shaft has become an urgent need. This document developed a brushless torque sensor built on strain measurement, which converts the torque into the deformation of the shell, and obtains the magnitude of the torque through the strain measurement of the shell. The experimental verification shows that the measurement error is less than 4%. When measuring the torque of the drive shaft of the cold rolling mill core, the number of torque oscillations is verified by the simulation of the inherent characteristics of the rolling mill transmission structure, and the torque amplitude statistics are determined by the engine power and speed signals. Practice has proved that the strain brushless torque sensor is achievable and the measurement result is correct, which provides a basis for torque detection works.

[6] Dieter Doerrie and Paul Schwerdt 2014 et al. The disc-shaped element has a first torque transmitting portion radially adjacent to the measuring element area on the inner side and a second torque transmitting portion radially adjacent to the measuring element area on the outer side. Compared with torque transmission components, the latter is a measuring element with a smaller axial thickness, which shows mechanical stress under the influence of torque. The axial thickness of the element decreases radially outward. Therefore, the strain gauge extends in a certain axial area and converts the mechanical stress caused by the torque of the measuring body.

[7] M. H. Muftah, S. M. Haris, 2010, etc. The most important variable of rotating machinery in this work is the mechanical active power, which is measured by directly measuring the torque on the rotating shaft and measuring the speed. The structure of strain gauge and strain gauge torque sensor is used for measurement. The structure of the mill was analyzed to take into account the torque measurement with strain gauges on it. The version with torque sensor is used with strain gauges. This study outlines the implementation of the converter. Use Spider8 PC measurement electronics to calibrate the sensor, the measurement chain block diagram, the most important points in the measurement software and catman ® Express software, measurement accuracy and sensor testing under simulated load.

The software attached to the computer instrument determines whether the system functions are convenient for users to use. The software is an integral part of many tasks to be performed that affect all aspects of the measurement process.

[8] Zhigang chu and Hongyu shu 2020 et al. This article describes the geometry of a strain gauge-based torque sensor; the measured torque must be converted into a uniform normal strain load. Disc torque sensors are widely used in robot joints and wheel drives. However, for traditional spoke geometries, there is always a trade-off among sensitivity and stiffness, because their load depends on the bending deformation mode that causes the uneven load. This article introduces the lever method of strain gage torque sensors, which executes uniaxial tension and compression modes to optimize strain uniformity and improve trade-offs. In addition, the F-type torque sensor proposed based on this method has the characteristics of axial thinness, simple installation of strain gauges, and flexible adaptation. Simulation and test results confirmed the basic design ideas.

[9] Min Li, Yu-Xiang Sun 2015 et.al., This torque sensor based on sectional redundant measurements, which can be applied to torque measuring of motor starting, running and stopping. The sensor can withstand an axial force of 1000kg while the interference from the axial load remains low. The maximum range is up to 400Nm. In order to ensure accuracy and rigidity, the entire measuring range is divided into three sections, since the moment of motor starting, motor running and motor stopping, the maximum torque of each stage should be approximately 400Nm, 210Nm, and 60Nm respectively. A wheel shaped elastic body with 8 radial beams on which foil strain gauge and semiconductor strain gauge are adhered and serve as the sensing unit. The combination of foil strain gauge and semiconductor strain gauge forms a redundant measuring system. It was found at lower range, the sensibility of the semiconductor gauge is superior to the foil gauge. But at higher range, the linearity drop of the semiconductor gauge results in lower measuring accuracy compared to the foil gauge. By using semiconductor gauge at lower range and foil gauge at higher range, we are able to achieve fair accuracy and linearity at the whole measuring range.

[10] Hong Liu, Yiwei Liu, 2014 et.al., This is a novel six-axis force/torque sensor based on strain gauges. Firstly, the six-axis force/torque sensor's design criterion is systematically expounded by calibration matrix, condition number, coupling error, sensor accuracy, strain gauge sensitivity, sensor sensitivity and sensor stiffness. Secondly, a novel sensing element is designed and simulated by finite element method. Then, the performance of the sensor is obtained by analysis. In the end, the sensor was manufactured.

[11] Dae-Han Hong, Jinung An 2012 et.al., In order for a robot to handle various objects and perform or assist the tasks of a person, the robot has to be similar to the hand of a human and manipulation tools with the same functions were necessary. To properly perform such object manipulation functions, research and development of manipulation tools with integrated sensor technology utilizing sensors are being pursued. Although the force-torque sensor is the most general among such sensor technologies, miniaturization is necessary in order to apply the sensor to an intricate manipulation tool such as that of the human hand. In this regard, this study is about the sensor frame design and analysis for the development of a miniature force-torque sensor.

2.2.2 Electronics / Electromagnetic phenomena

[12] Vischer and Khatib 1995 et al. Faraday's law (inductive sensors), magnetostriction and magnetoelastic effects are used for electromagnetic sensors, and linear variable differential transformers (LVDT) are used for torque sensors. The spoke structure of the torque sensor has a flexible support, an LVDT. The main advantages of LVDT are its high robustness, excellent resolution of approximately 0.1 μm , good accuracy (0.010.3%), and simple installation and calibration. High reliability stems from its working principle, which is based on magnetic transmission, which eliminates physical connection between sensor elements. The close relationship between the magnetic core position and the output voltage of the secondary coil results in excellent resolution. Inductive sensors will experience signal attenuation at very low frequencies and will be affected by electromagnetic noise. The smallest LVDT weighs only 4.36 g and has an outer diameter of 4.77 mm, but its 22.4 mm length makes the compact overall dimensions of the torque transducer.

[13] Shinoura, 2003, etc., the effect of the change in the magnetization caused by the tension applied to the material is called the Villari effect or magnetostriction. The magnetostrictive torque sensor is composed of a rotating shaft having a herringbone magnetostrictive metal layer formed on the shaft, an output coil, and a pickup coil for detecting changes in the magnetic properties of the magnetostrictive layer. When alternating current is applied to the excitation core, the magnetostrictive layer is excited. The torque applied to the magnetostrictive element generates stress. Due to the Villari effect, the permeability changes and generates an inductive output in the pickup coil when a torsional load occurs. The advantages of this sensor are the non-contact contact between the shaft and the housing and great torsional stiffness. The disadvantages are complex production, heavy structure, strong magnetic shielding, and insufficient performance (linearity of 3-5% FS, hysteresis of 2-3%, resolution of 10 mV/V).

[14] In this article, Hubert Gattringer and Andreas Muller proposed two alternative sensor concepts for indirect measurement of end effector (EE) load in 2021. Both sensors are located on the robot base. The first sensor design includes three load cells mounted on the robot. The second concept consists of a steel plate with four spokes hanging from it. Strain gauges are attached to each spoke to measure local deformations related to the load on the sensor plate (similar to the main principle of force-torque sensors). Deriving the EE load from the basic keys determined in this way requires the dynamic model of the robot to consider static and dynamic loads. The prototype implementation of these two concepts is reported. Special attention is paid to model-based calibration, which is essential for these indirect measurement concepts. When using a new sensor, the results of the experiment will be displayed.

2.2.3 Optical domain

[15] Hirose and Yoneda 1990 and so on. Made a significant contribution to the research of optical force/torque sensors. They suggested using a split grating to detect the movement of the light source (LED) due to the force applied in two directions and the flexible part of the optical sensor. Photoelectric sensors have

shortcomings such as non-linearity and temperature sensitivity, but compared with other sensors, they are more reliable, cheaper, and simpler in design. The offset is detected by interrupting the light between the light source and the detector, changing the intensity of the reflected light, or by the relative displacement of the light source and the detector. The sensor has a force adapter board, load cell (elastic element), photodetector, LED and mounting adapter board. When force is applied to the plate, the elastic solid deflects the LED light falling on the grating.

[16] Takahashi 2003, Okutani and Nakazawa 1993 et al., Nara Institute of Science and Technology developed a 6-axis optical force/torque sensor for fMRI applications. The sensor is made of acrylic resin to exclude any metal sensor components that may generate fMRI signal noise. In this design, the elastic frame has a Y-shaped topology with S-shaped rods to allow the active area to move 6 DOF. The force applied by the user deforms the elastic frame and changes the intensity of the light falling on the optical fiber. The torque measurement accuracy of this sensor is 2.65%. The converter is very complicated and only suitable for narrow applications. The idea is to calculate the torque by using an optical encoder to measure the torsion angle of the torsion shaft to detect the difference in the rotational positions of the disks on opposite sides of the torsion shaft. Encoder-type torque sensors have a large overall size and require very precise perforated disk installation. To overcome this problem, the author (Horton, 2004) invented a torque sensor that has a light source, a two-dimensional radiation detector array, and two modulating perforated disks arranged between the light source and the detector. When torque is given to the shaft, the relative position between the discs will change the overlapping grooves, thereby changing the aperture size that controls the light pattern incident on the optical detector.

2.3 Literature Outcome

Different working principle studies based on different design through which some of them are used to particular or specific use application and some of them are for universal use provided valuable knowledge regarding different torque value capturing methods and also design studies helped to structure design fundamental

according to working parameters where the new torque transducer is going to be used. The various operation principle from electrical domain, electronics / electromagnetic domain and optical domain each of the principle having its own advantages and disadvantage for the specified application where it is going to be used. So comparison all of them based on their advantages and disadvantages is as shown below.

Parameter	Electrical	Electronic/Electromagnetic	Optical
Operating Principle	Simple, easy to understand	Quite simple but requires expertise for particular application use	Complex for understanding and use for small applications
Cost	Lower in comparison to other	Moderate cost but lower than optical	High cost of manufacturing
Data transmission	Through slip ring and brushes	Through signal conditioning and processing unit	Sensed by photointerrupter/Photosensor and calibrated at central processing unit
Output	Amplified through amplifier and displayed in mV	Processed and converted through IC and CPU and displayed	Processed through local impedance control system and displayed
Common applications	Widely used for motor, gearbox and pump torque testing	Mostly in automotive applications such as engine transmission testing	Mostly for robotic application as cost is on higher side.

Table 2.1: Comparison study of different principle of torque sensors

Through literature review, it has been observed that much work is done on torque sensor working on different principles, but still with requirement of different application base as well as the industries are moving towards the use of automatically or numerically operated machineries, developing the torque sensor for particular or unique application. There is scope of developing a torque sensor considering different working parameter improvements with respective to working conditions.

The electrical principle based strain gauge torque sensor is considered for design and development as it is most commonly used in applications such as motor, gearbox and pump torque testing and can be manufactured at an controlled cost for universal use application where inline shaft to shaft torque measurement is required.

Also through literature it is evident that there are very few truly Indian manufacturers of rotary torque sensors in India, those companies either works in joint venture with NRI firms or trade that technology from outside for example Sushma industries Bangalore, Sense India Jaipur, adiartech (joint venture with artech

USA) transducers Gujarat. Most of the manufacturers present in India such as Kistler Holdings (Switzerland), Honeywell International (USA) and many more are NRI companies who operate in India and import the sensors from outside India or their home country because of which the cost of their products per piece is high (in a range 1 lakh to 2.5 lakh). There is a scope of developing and manufacturing those products in India locally to cater the high price. Below is the price range of rotary torque sensors of different manufacturers is listed below;

Manufacturer (country)	Price (rupees)
Futek (USA)	1.7 lakh
ABB (Switzerland)	1.5 lakh
Crane electronics (UK)	1.2 lakh
Kistler holdings (Switzerland)	1 lakh

Table 2.2: Torque sensor manufacturers and its prices

2.4 Problem statement

In today's modern era in order to modify and upgrade technology, cost plays an important role for accessing that technology, therefore designing and developing a rotary torque sensor by improving the performance characteristics in accordance to the relative positioning changes and to work with respective working conditions ranging from temperature change to external forces more efficiently. There is need to study those aspects of developing the sensor with improvisation in the performance.

In most cases, torque sensors are used for strain measurement, clutch and gear testing, and dynamic torque in engines. In addition, the powertrain, braking and suspension systems are all tested with torque sensors, which are also used to measure performance to improve fuel efficiency. Therefore the rotary torque sensor is selected for the design purpose by improving its performance characteristics and considering the cost factor and to manufacture it in MAKE IN INDIA policy in near future for making India a truly ATMNIRBHAR country.

2.5 Objectives of present work

1] To study various working principles and operating methods of different types of torque sensors.

- 2] Determine methodology and select best suitable working principle by considering performance characteristics such as working environment, nonlinearity, hysteresis, rotational speed and rated output.
- 3] Prepare conceptual design and develop it according to specified performance characteristics and perform its finite element analysis.
- 4] To check the manufacturing feasibility with best suitable manufacturing technique at controlled cost for accurate torque value measurement.

Chapter 3

Design and Specifications

3.1 Design Fundamentals

Below is the list of different dimensions details and components of rotary torque sensors from different manufacturers for a 100 Nm capacity.

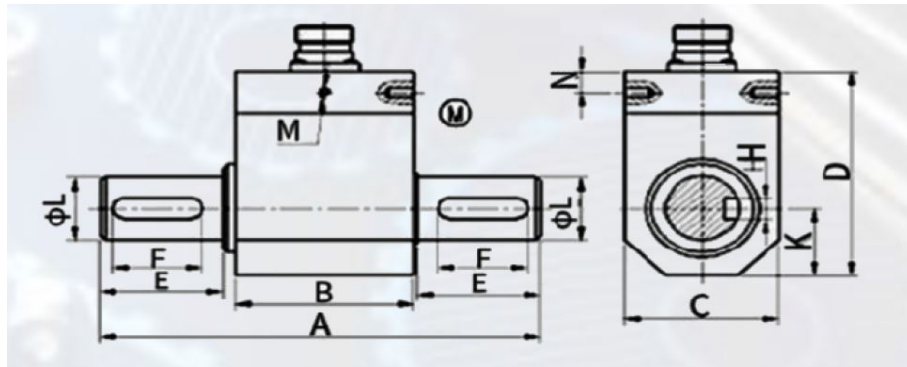


Figure 3.1: Torque sensor dimensions

The range of dimensions of various manufacturers is used for the reference while looking for proposed design of different parts of the inline torque sensor. Such as, design of shaft which is the core/ principal part in the sensor (on which the strain gauges to measure deformation are to be mounted), Design of housing is prepared by considering the space for other parts/ geometries of the whole sensor as a unit.

Sr. No.	Manufacturer	A	L	B	C	D	E	F	K	N	M	H
1	HBM	108	19	44	38	58	30	22	19	6	3M3	6
2	Futek	114	22	48	42	58	32	24	22	6	3M4	6
3	Kistler holding	126	25	52	48	56	36	28	28	6	3M3	6
4	Honeywell international	138	28	54	52	57	39	30	33	6	3M3	6

Table 3.1: Dimensions of Rotary torque sensors

3.2 Design of shaft

During the design of shaft, it is done by considering the higher range of dimensions to further optimize it by finite element simulation process. As the core part/Principle element is the shaft so while designing it the main aim is that it should have an optimum size that doesn't look too big for the desired torque capacity or too small for desired torque capacity and fail under the working range and avoid the undersized/ Oversized phenomenon. The whole process of optimization is discussed in point 3.3 in FEA analysis. This design is considered and optimized for SS304 material properties and considering the factor of safety as 1.5 to the rated/ required torque capacity for which it is designed i.e. 100Nm. And the speed of rotation as 3000 rpm max.

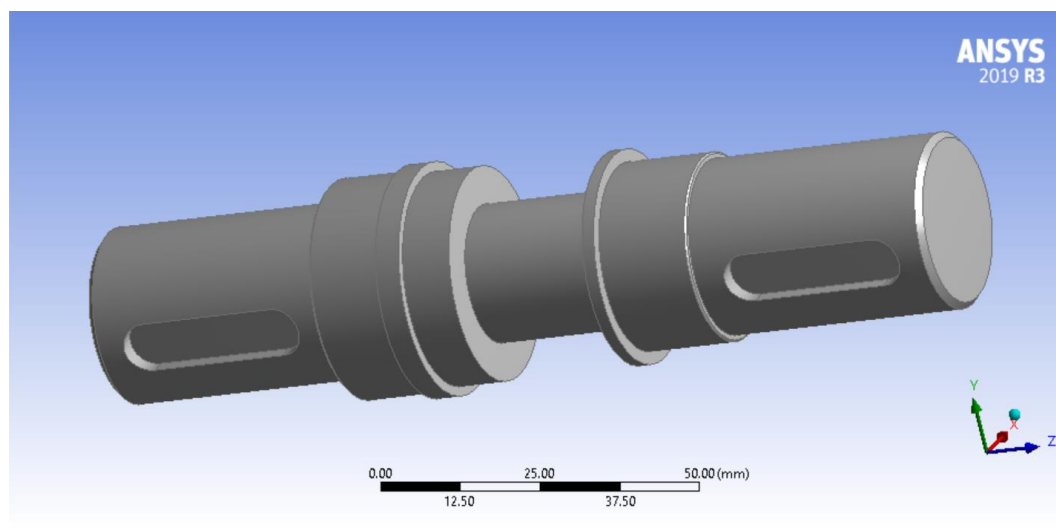


Figure 3.2: Design of shaft

3.3 Finite Element Analysis of Shaft

Boundary conditions used during FEA process are as shown in figure.

(a) Fixed Support: - Fixed Support is used on one end face of the shaft as shown in fig 3.3 as a boundary condition so as to hold shaft from one end.

(b) Cylindrical Support:- Cylindrical support is applied to the shaft at the place where bearings are supposed to be mounted. In this the axial movement and tangential movement is fixed as it is not desired to happen but radial movement is kept free as like a bearing so that shaft is supposed to rotate when torque (moment) is applied.

(c) Moment: - The moment is applied on other end face of shaft as shown in fig 3.3 to apply desired torque values from that end to the shaft.

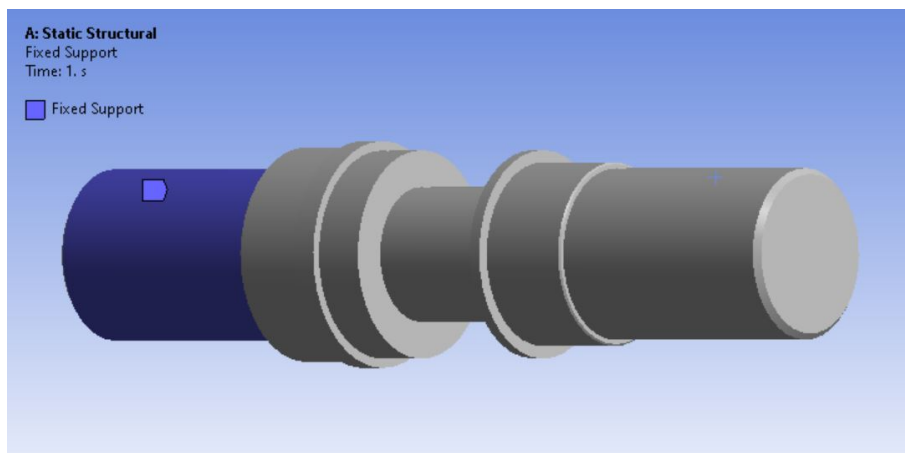


Figure 3.3: Fixed Support Boundary conditions used during FEA

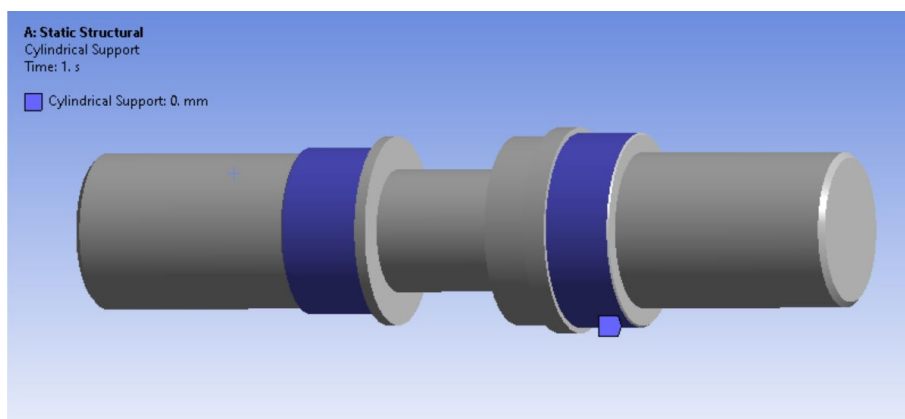


Figure 3.4: Cylindrical Support Boundary conditions used during FEA

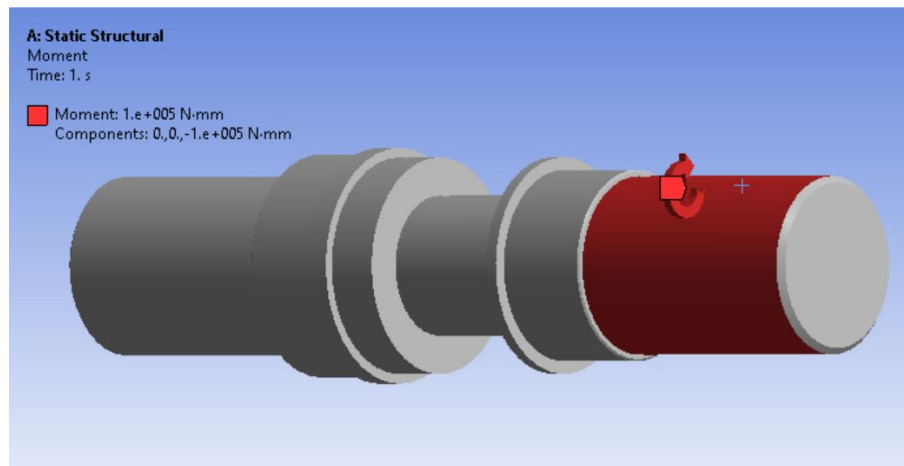


Figure 3.5: Applied Moment Boundary conditions used during FEA

3.3.1 Oversized Shaft Condition

During the design stage and FEA simulation at first step we considered higher range of dimensions (Sr.No. 4) from reference dimensions as shown in table 3.1. The selected material properties of SS304 steel are given and analysis is performed. The analysis was successful over 200 Nm also there is no generation of plastic state. But our aim is to design a compact sized sensor and it is for 100NM. So then we reduced the dimensions stepwise to find a more compact sized shaft and termed this as oversized design. Oversized Shaft Condition is shown in figure 3.6

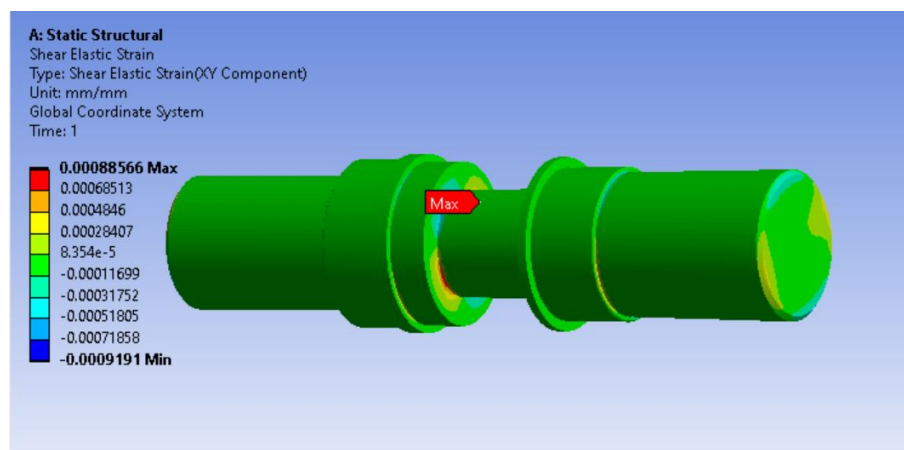


Figure 3.6: Oversized shaft design condition

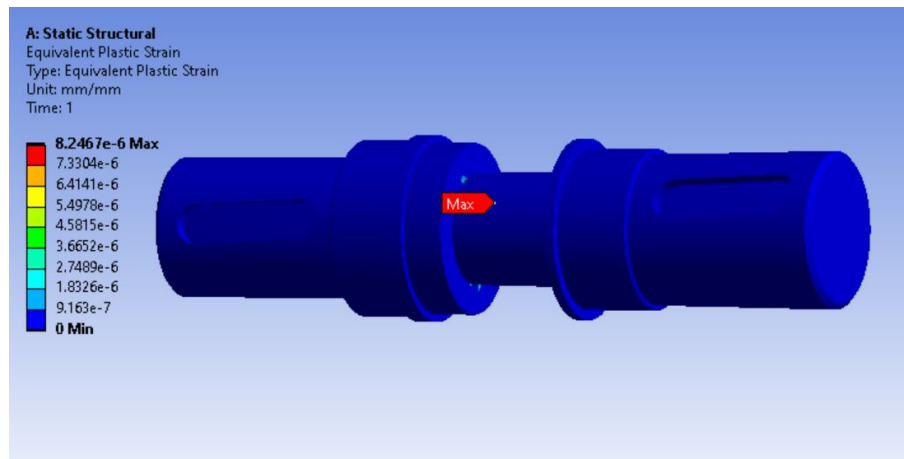


Figure 3.7: Undersized Shaft Condition

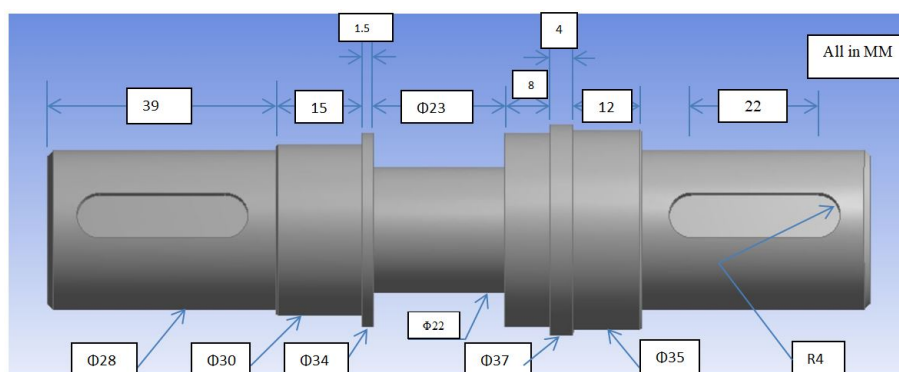


Figure 3.8: Optimum Shaft design condition

3.3.2 Undersized Shaft Condition

In order to further optimize the dimensions we reduced the dimensions to a level where the shaft has become compact in size but at the required torque capacity and considering FOS as 1.5 and material properties of SS304, there is generation of plastic strain in the shaft which is ultimately a Failure stage in design and safety parameter as considered for rated 100Nm design and development. Undersized Shaft Condition is shown in Figure 3.7

3.3.3 Optimum Shaft Design

The Optimum design condition is based on the rated torque capacity of 100 Nm with FOS as 1.5 and Spaces assumed for other essential parts mountings. With this design of shaft is completed and required results for torque range from 0 Nm to 100 Nm are plotted. Optimum Shaft design condition is shown in Figure 3.8

3.4 FEA for optimum design shaft

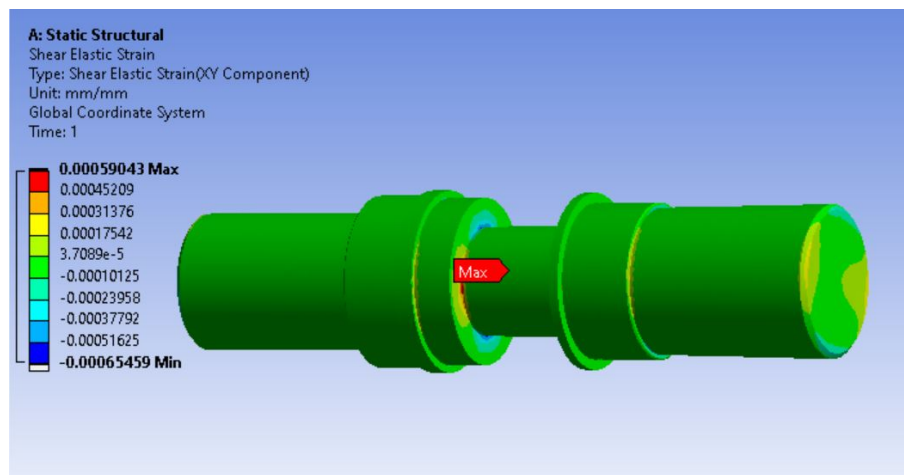


Figure 3.9: Ansys strain results for optimum shaft design

3.4.1 Ansys Strain Results

As shown in Figure 3.9. Finite Element Analysis is performed on Shaft to find shear strain results for torque upto 100 Nm capacity at interval of 10 Nm from 0 Nm to 100 Nm and results are noted. Shear strain results are actually to be measured through strain gauges and calibrated in terms of torque value. These shear strain results are taken for desired steps and plotted in table 5.5

3.4.2 Ansys Stress Results

As shown in Figure 3.10. Finite Element Analysis is performed on shaft to find shear stress results for torque upto 100 Nm capacity at interval of 10 Nm and results are noted. Shear stress results are taken just to check them with analytical results that are calculated through mathematical formulation process and also to find high and low stress location in shaft on loading. The results are taken for desired steps and plotted in table 5.5.

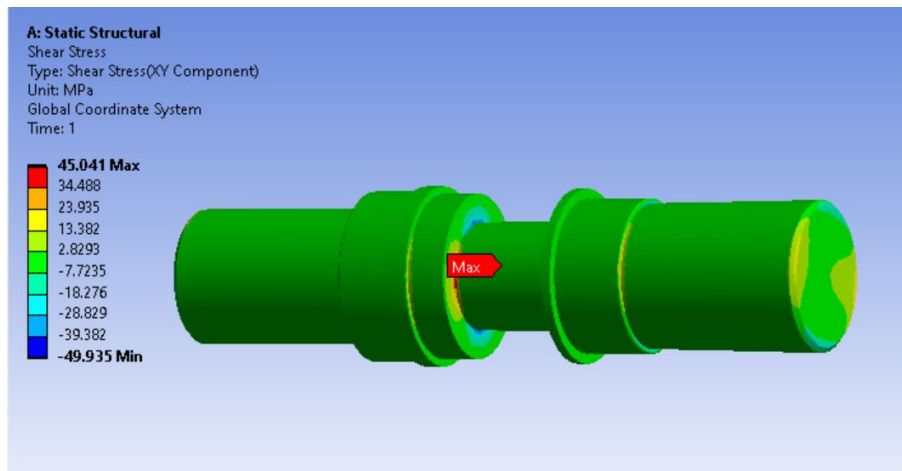


Figure 3.10: Ansys stress results for optimum shaft design

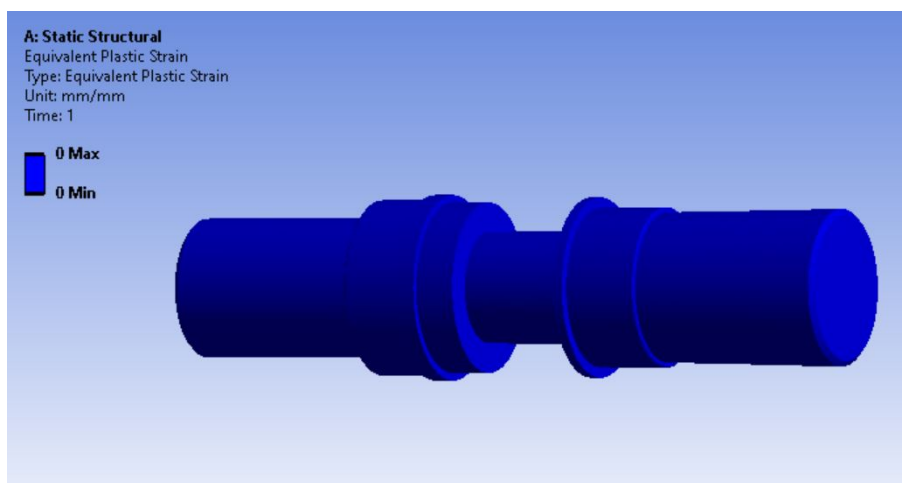


Figure 3.11: Ansys plastic strain results for optimum shaft design

3.4.3 Ansys Plastic Strain Results

As shown in Fig 3.11. Finite Element Analysis is performed on the shaft to find plastic strain development in the shaft. Through results there is no generation of plastic strain upto rated capacity of 100 Nm. as shown in fig.3.9. The plastic strain development starts after 150 Nm. The plastic strain development is necessary to check because once the shaft goes into plastic state even after the load removal then it will be a failure state of sensor. Also by considering the FOS as 1.5 the criteria for safety also fulfilled and design optimization of shaft is completed and considered for manufacturing.

3.5 Signal Transmission System

When the manufacturing of shaft is completed and strain gauging is done there will be a need of signal transmission from the work location to a remote/ central space where the results are monitored or taken into account. To satisfy this need of signal transmission Slip ring and brush assembly is considered for this torque sensor. As slip rings can be directly mounted over the shaft in connection with the strain gauge circuit and have continuous rotation as the shaft rotate. And excitation voltage to the gauge and output signal from the gauge can be given/taken with the help of brushes in contact with slip ring.

3.6 Bearing Specifications

There are two bearings which are supposed to be used for the support of shaft in order to rotate the shaft within the housing of the whole sensor and without any other positional changes within the assembly. The selected bearings are from standard bearing data book of type single row deep groove ball bearings having bearing number 6906 and 6807 in the universal standard data for bearings. The dimensional specifications of the bearings are as shown in figure 3.12.

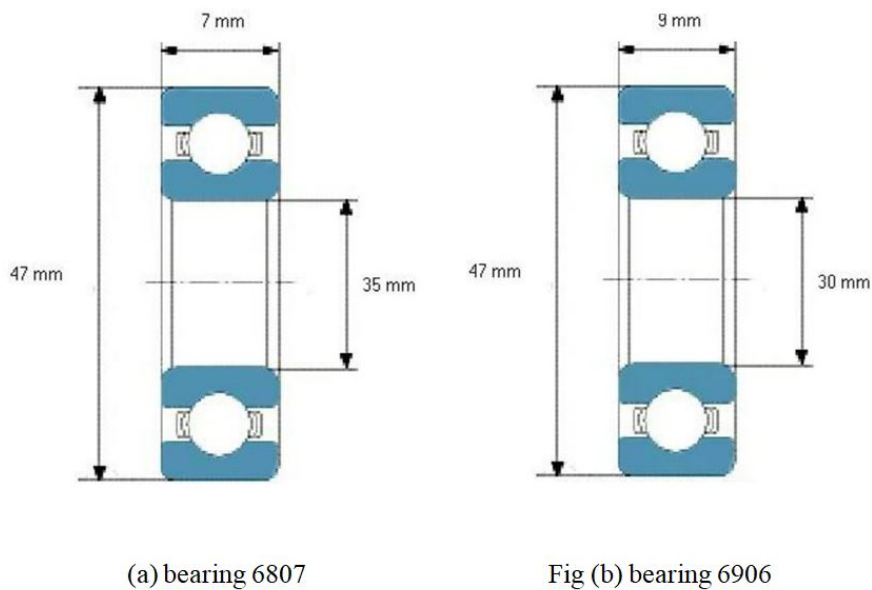


Figure 3.12: Bearing Specifications

3.7 Sensor Housing Design and Proposed Assembly Setup

During the literature study most commonly available sensor have their casing material as Aluminium. As aluminium is better for machining with lower cost and some of its alloy also have good hardness. during the design of casing and its cover aluminium of grade 7075 is taken into Consideration. The sensor housing design is completed by considering spaces for each and every component from the torque sensor. This design of sensor housing includes spaces for shaft and bearing, space for slip ring and brushes circuit mounting as well as the clearance space for the slip ring assembly and the circlip to hold the whole assembly tight without any kind of unnecessary movement of sensor Components. During the design it is also considered for a better insulation and environmental protection that dirt or dust should not enter into the sensor. The housing design is shown in fig.3.13 and fig 3.14 also the sensor housing cover plate with connector slot is shown in fig 3.15 and fig 3.16. after including all of its components sensor will have a proposed look as shown in fig.3.17. the Whole setup as exploded view of the assembly is shown in figure 3.18.

The Housing Cover plate design is shown in figure 15 and figure 16 which also has an hole where a electrical pin is supposed to be mounted to connect it with DAQ system to capture the data of torque.

This proposed final design includes the necessary components which are required to complete the torque sensor as a single product unit. This includes Shaft along with bearing and slip ring with brush assembly for signal transmission.

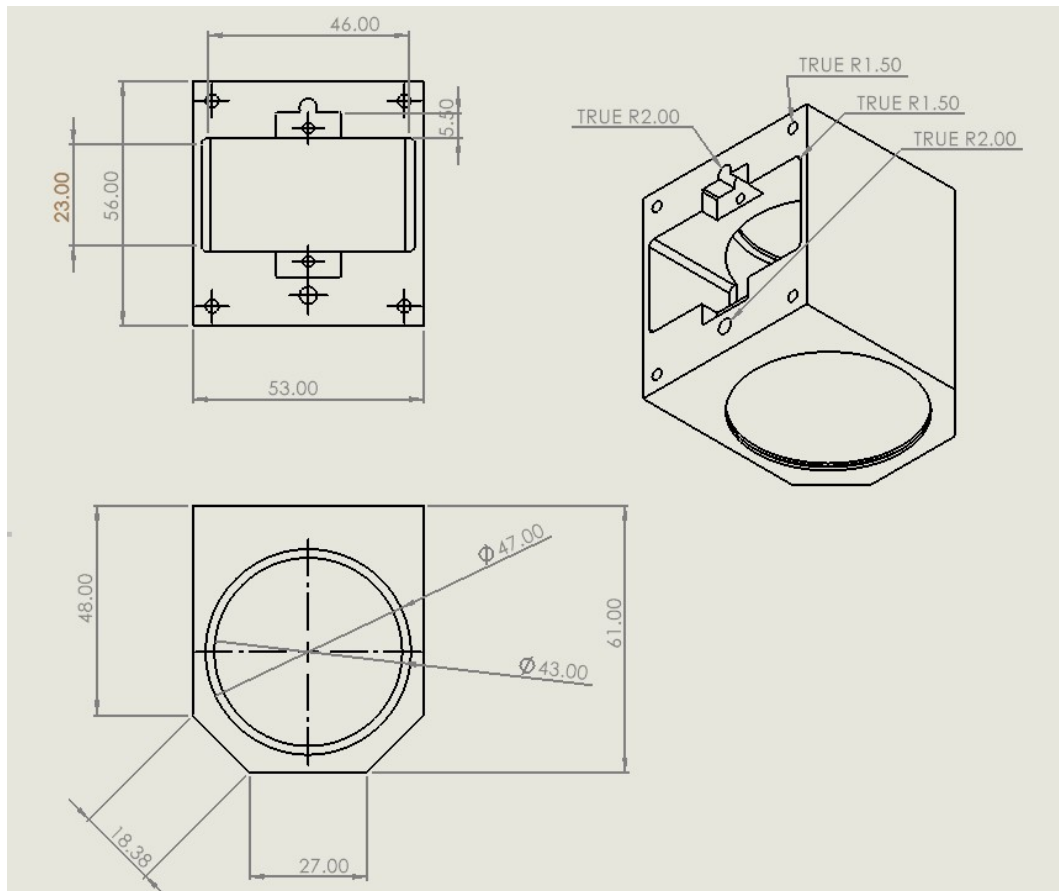


Figure 3.13: Sensor Housing dimensions

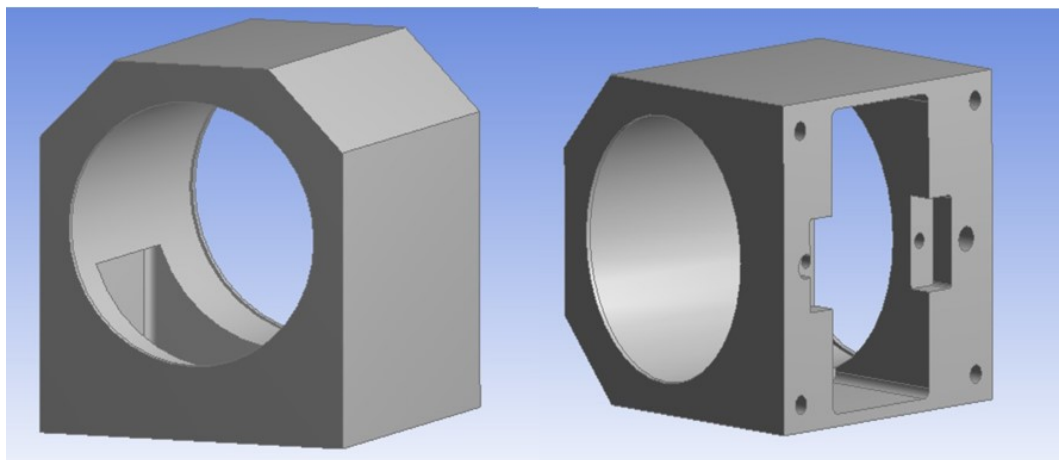


Figure 3.14: Sensor Housing Design

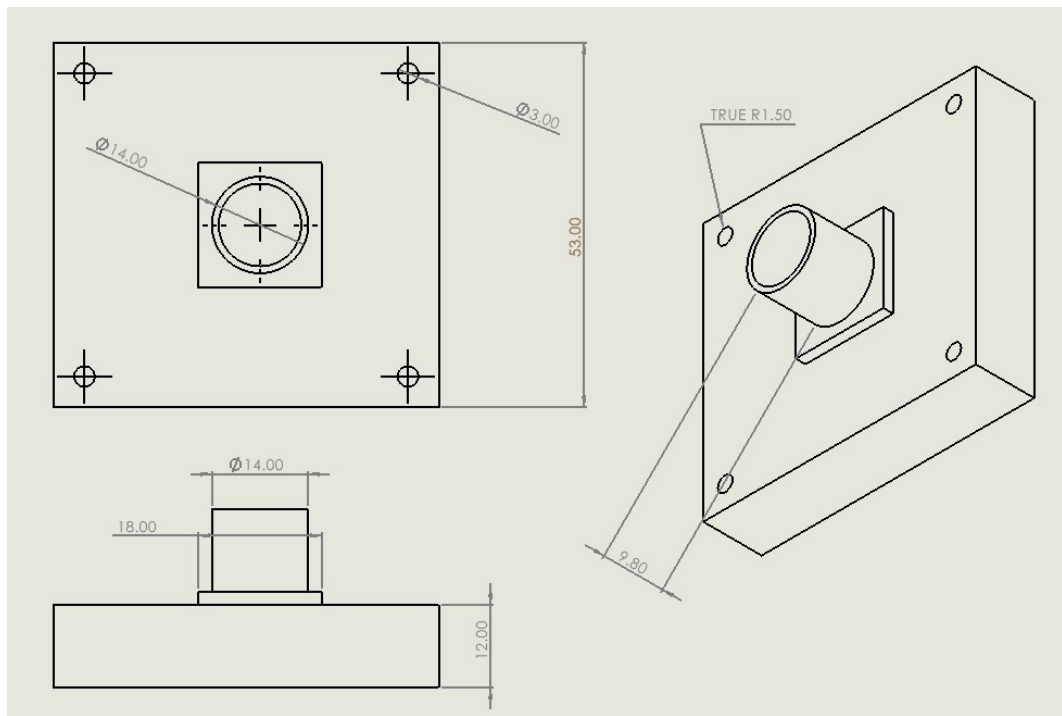


Figure 3.15: Casing cover plate with connector dimensions

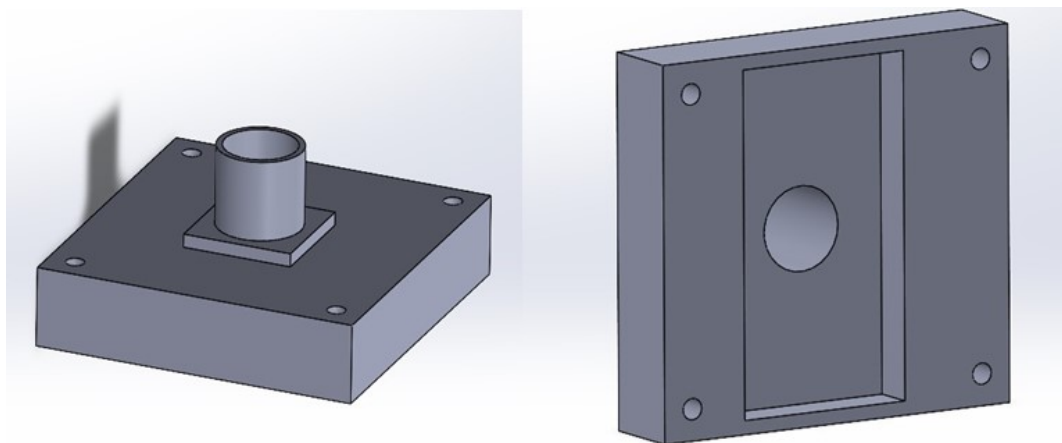


Figure 3.16: design of Cover plate with connector

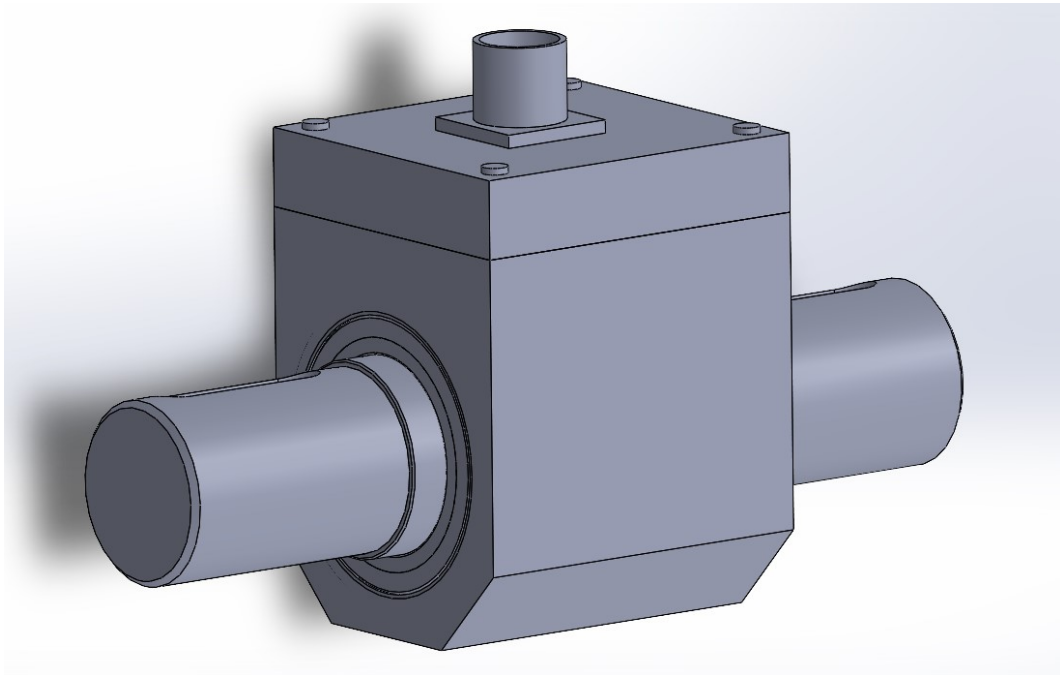


Figure 3.17: Assembly view of sensor

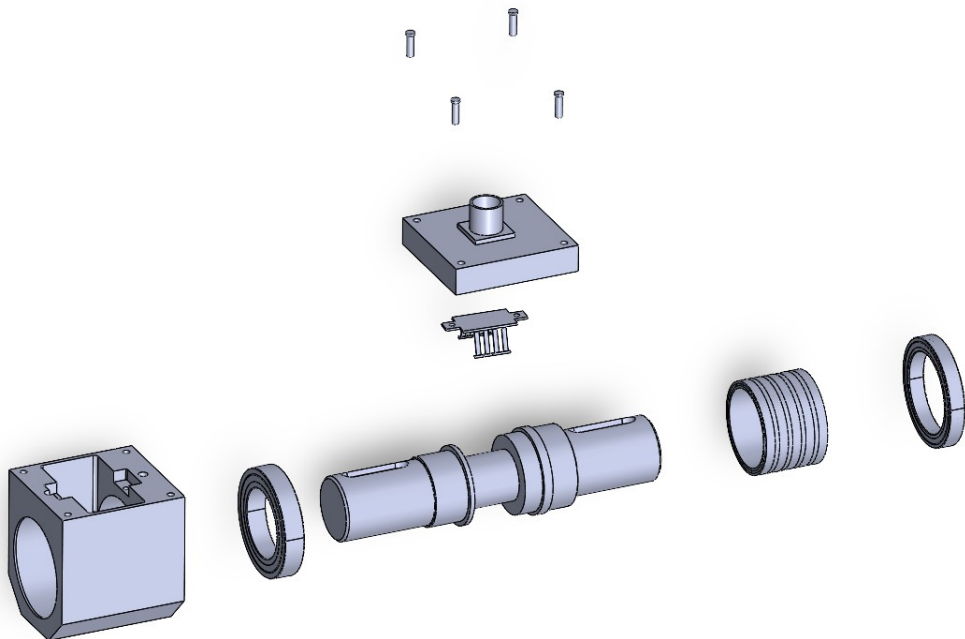


Figure 3.18: Exploded view of sensor

Sr. No.	Description	Quantity
1	Sensor Shaft (SS304)	1
2	Bearing 6807	1
3	Bearing 6906	1
4	Screw (3mm)	4
5	Screw (2mm)	2
6	Sensor Housing	1
7	Housing Cover Plate	1
8	Strain Gauges	2
9	Slip ring and Brush Assembly	1
10	4 Pin Connector	1

Figure 3.19: BOM and the quantity of components required for the sensor to be a end product

Chapter 4

Experimental Work and Calibration

4.1 Strain gauging Selection

Usually, torsion expresses the principal stress as shear stress, so it is necessary to measure the cause shear stress. In this case, when the torsional stress of the circular shaft is detected, the main expansion direction is recognized as being at $\pm 45^\circ$ from the axis of the shaft direction. The main function of a metal strain gauge is usually to generate strain through the resistance of an electrical conductor. In this work the Y-shape gauge or torsion gauge from National Instrument and Engineering, Jaipur, India is considered as shown in Fig. 4.1 With the measuring grid axes are at $\pm 45^\circ$ to the axis of symmetry.

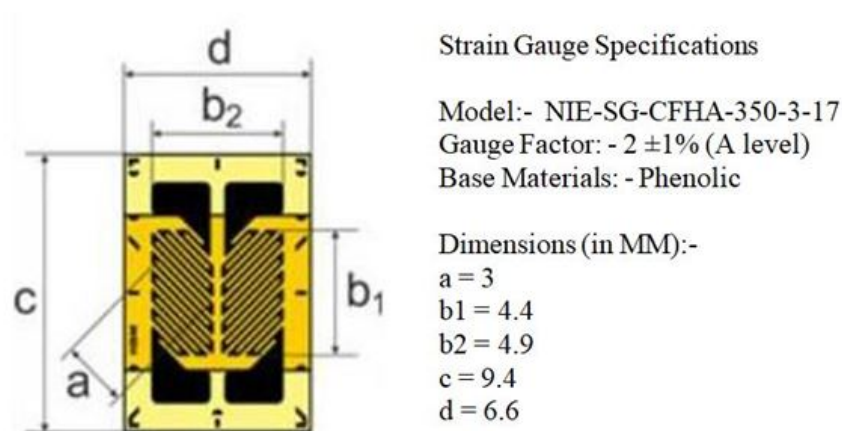


Figure 4.1: Strain gauge details

Overall, this strain gauge is small in size and shape, not much costly, easy to attach, and the sensitivity is high to sense the strain but unresponsive to ambient or process temperature variations. During the experimentation the measuring axes must relate to the main stress directions for high level of accuracy and precision in results. Fig. shows a metallic strain gauge with the measuring grid.

4.1.1 Strain Gauge Circuit Connections

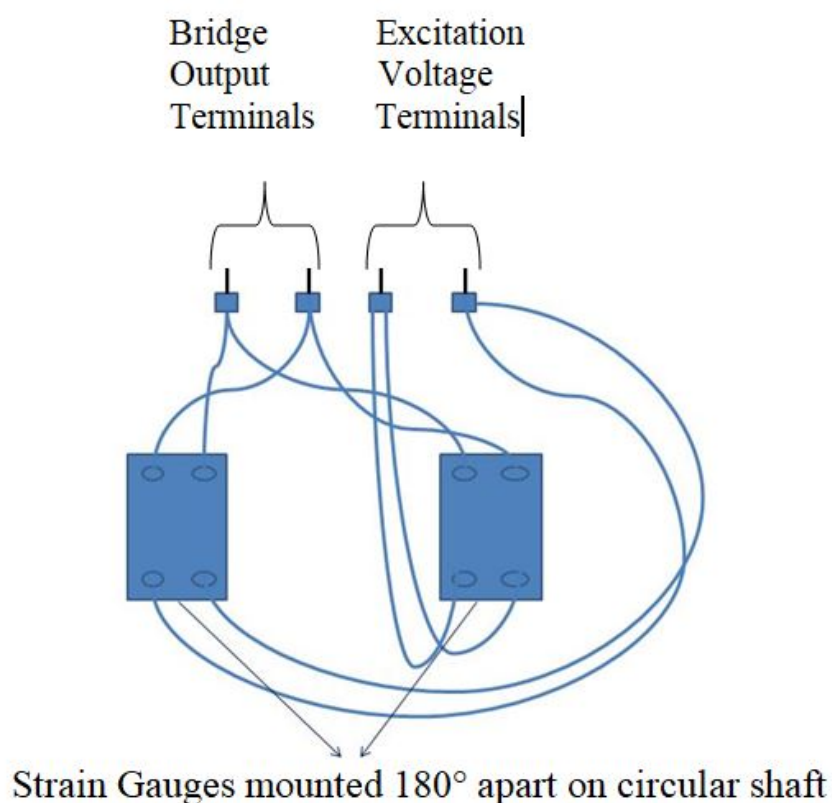


Figure 4.2: Strain Gauge Circuit

This is a gauge connection in the form of Wheatstone bridge circuit to be formed after gauge pasting on shaft.

4.1.2 Manufacturing of Sensor Shaft

The Optimum designed shaft is manufactured with use of CNC machine then it is followed through grinding process to have a better overall surface finish. And the middle portion of shaft on which strain gauges are supposed to be mounted is followed through buffing process so that there is no any kind of surface roughness

and have a super smooth surface for gauge pasting



Figure 4.3: Manufactured Sensor Shaft

4.1.3 Strain Gauge Pasting

If the gauge is placed accurately and conforms to the torsion characteristics, the system will be temperature compensated and will not be sensitive to bending, thrusts or pull. Therefore, any change in resistance is purely due to the torsion of the shaft.

Strain gauge pasting process is followed as,

- The first step for strain gauge pasting is cleaning. The surface where the strain gauge is to be mounted is cleaned by using cleaning agent. RMS1 spray from HBM is used as a cleaning agent. RMS1 spray is a mixture of acetone and isopropanol. With use of this cleaning agent any kind of small dust particles are removed. Then cellulose pads are used for wiping off any remaining particles and liquid compound.

- After cleaning the surface the marking at exact location such that the axis of shaft coincides with vertical axis of gauge and foils of gauge makes 45 degree

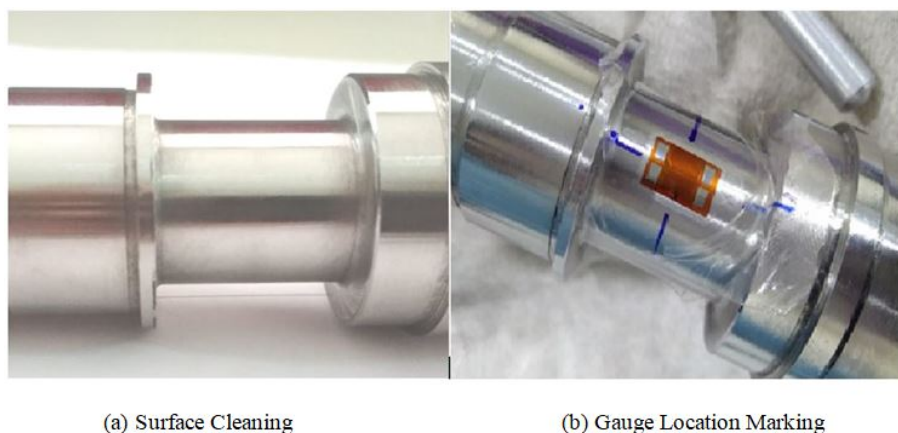


Figure 4.4: Surface Cleaning and Gauge location marking

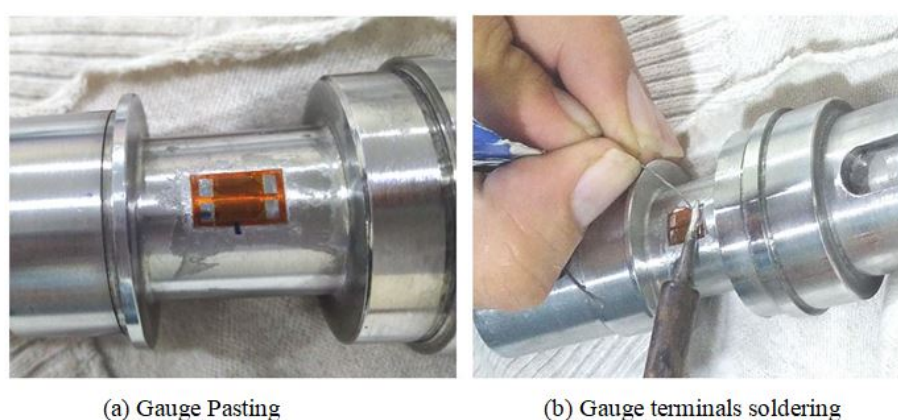


Figure 4.5: Strain gauge pasting and Soldering

angle with axis of shaft is done by a fine pointed marker pen.

- Then by applying a drop of adhesive to the back of strain gauge it is prepared for pasting. In this case X60 from HBM is used as adhesive as it is very easy to use. X60 consists of methylmetacrylate and it is free from dicyclohexyl phthalate which makes it useful for using it at wide range of temp from -200 degree to +150 degree and can be applied over very smooth metallic surfaces and cures in minutes.
- After that gauge is pasted over the shaft surface at exact location marked earlier by fine pointed pen and a small polyethylene sheet is used to cover the gauge and gauge is pressed by thumb for a minute to stick with shaft surface properly. After that gauge is visually inspected to insure that it is fixed properly on shaft surface and polyethylene sheet is removed.
- Then the wires are bonded to gauge terminals in order to complete a Wheatstone bridge circuit and connection are made for input and output terminal

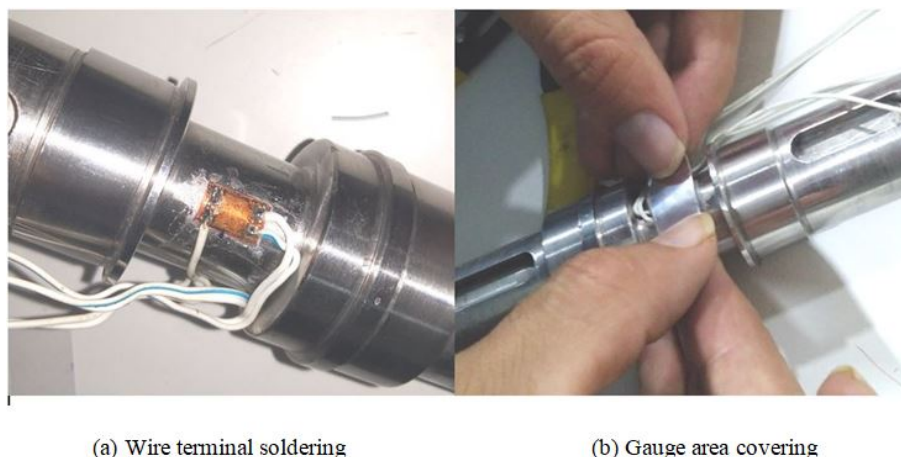


Figure 4.6: Gauge wire soldering and Gauge area covering

- Then with the help of Multimeter the wire terminals are checked to ensure correct circuit connections were made by measuring the resistance (i.e. 350 Ohm) and cross terminal resistance (i.e. 260 ohm).
- At final stage the whole gauge area setup is covered by wrapping a plastic electrical tape over it to ensure no dust/dirt particles enter to gauge area and to avoid any kind of damage to gauge during experimentation.
- The whole setup is then kept for 60 minutes for complete curing of adhesive to get best possible results.

4.2 Experimentation on Setup

4.2.1 Torque Setup Specifications

The whole setup for application of torque on shaft for experimental calibration as shown in fig includes two adapters for holding the shaft, loading arm with magnetic controlled motor, load cell and its controller.

This setup has a capacity to apply torque from 0 Nm to 45000 Nm at any desired steps. The applied load is multiplied with loading arm radius as shown in yellow color in above fig. the loading arm radius is 0.5 meter, this dimension is from center of object holding adapter to center of vertical loading bar. The whole setup with all necessary mountings is shown in figure 4.7

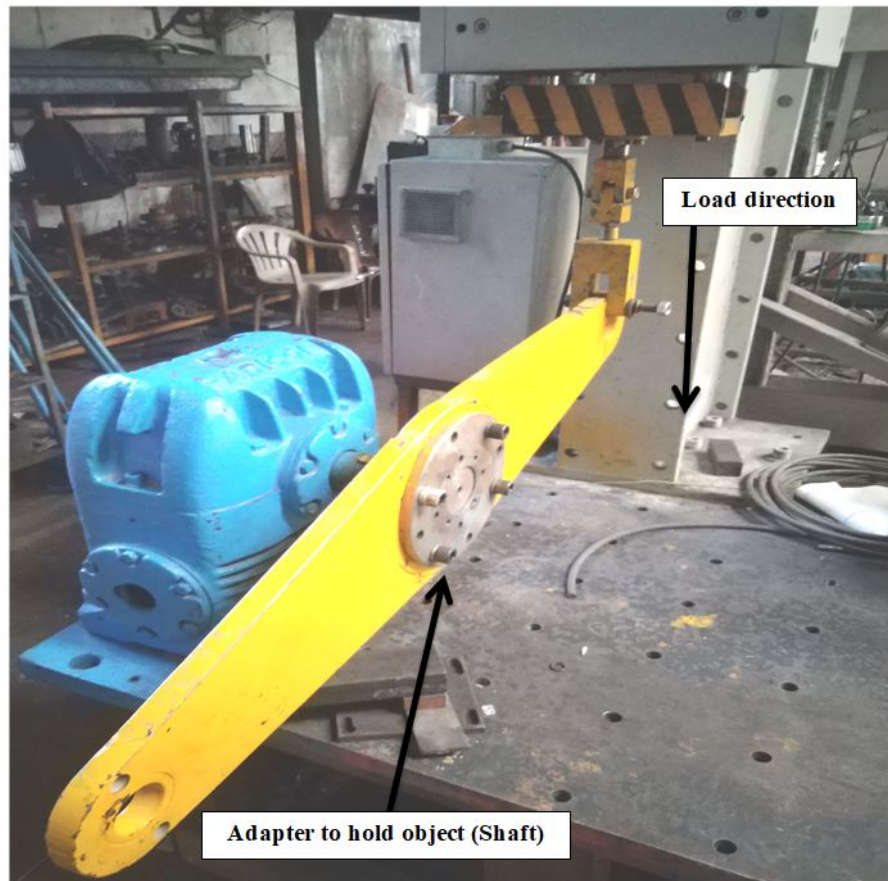


Figure 4.7: Experimental Setup

4.2.2 Experimentation

The experimentation process is followed as,

- First the two adapters were machined according to shaft diameter and keyway slot so that shaft is held properly in the flanges of torque application setup.
- The strain gauged shaft is mounted properly in the adapters with the help of key for proper fixing the shaft in adapters.
- The input as excitation voltage of 10 V is given to strain gauge circuit then the wires from gauge terminals are connected to e-DAQ and data storage module, the load cell is connected to its indicator and controller. This whole setup including motor controller for precise load application acts as data acquisition system and it is ready to apply controlled torque.
- The torque application process is gradual and stepped in the interval of 10 Nm from 0 Nm to 100 Nm such that ten steps of torque are applied.
- For first step the load is being applied through magnetic motor with help of its controller and simultaneously the applied load is being measured and calibrated

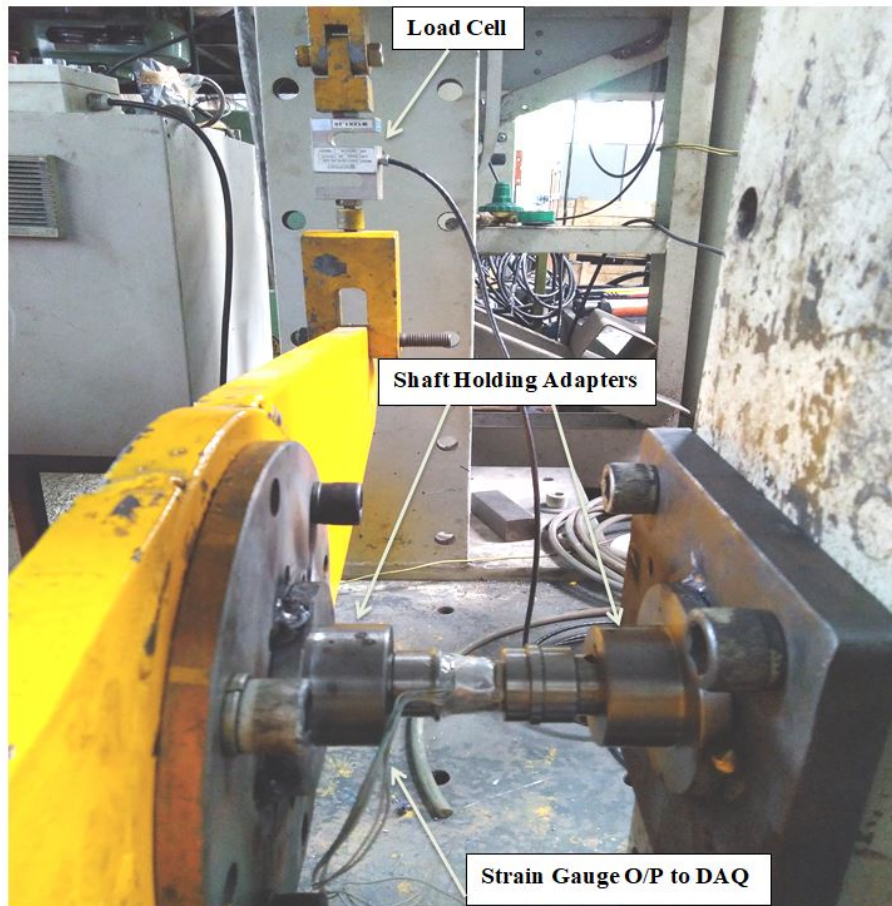


Figure 4.8: Experimentation on Shaft

with the help of load cell mounted on loading arm.

- As load is applied with loading arm is in kg, torque value is calculated with the help of applied load multiplied by gravity into load arm radius in meters in the system.
- So the output generated from strain gauge is transferred to e- DAQ calibrated in millivolts and being stored in data storage module.
- Similarly for each step of 10 Nm upto 100 Nm the same process is followed and results are recorded and result file is generated.
- To check repeatability of reading results the whole process is carried out for three iterations and the results are noted and inspected.
- At the end the results are plotted in excel sheet and graphs are generated.

The Data acquisition system includes somet e-DAQ, display unit and data storage module

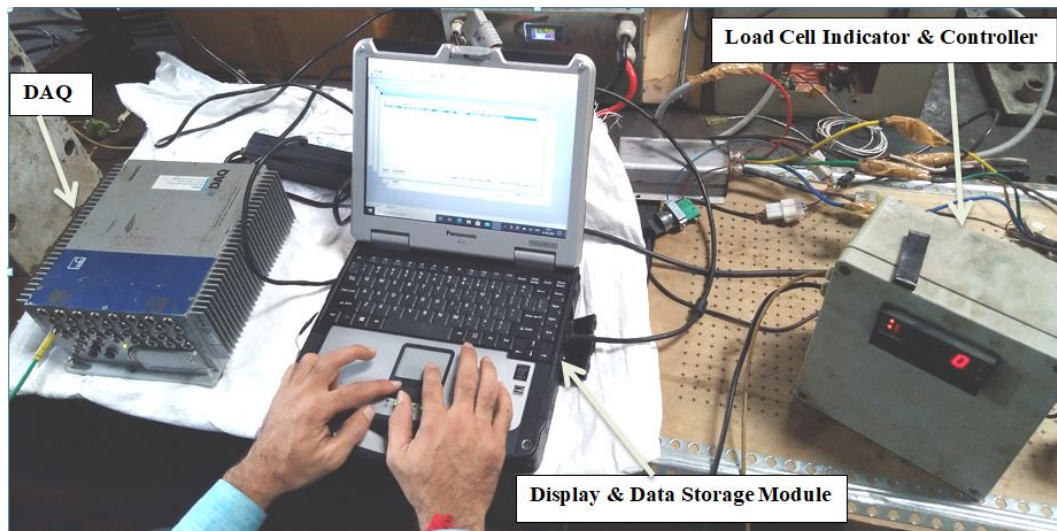


Figure 4.9: Data Acquisition Setup

4.2.3 Data Acquisition System Specifications

The e-DAQ is the perfect instrument when testing any number of applications, containing agriculture, construction, mining, automotive, recreational vehicles, military and much more.

The e-DAQ is a layered system containing of a base processor that can support up to 8 signal conditioning layers. In these there are four layers (e-DAQ EHLS layer, e-DAQ EBRG layer, e-DAQ EDIO layer, e-DAQ ENTB layer) that can be used for strain gauging work depending upon the application complexity and amount of signal conditioning required, and the signals can include CAN, bridge, temperature, pulse, voltage and more.

The e-DAQ EBRG layer is used in this experimentation process as the gauges used and circuit is not so complex and it is best suited for simple to medium complex strain gauging work.

It is 16 channel bridge layer,

- Strain gauge (full, half and quarter bridge) inputs
- 350 Ohm and 120 Ohm capacity gauges can be used simultaneously
- Provides digital output

The processor used is e-DAQ (ECPU PLUS COM) is an upgraded processor for the e-DAQ signal conditioning layers that have memory upto 256 gb, 3 CAN and 1 GPS Ports and supports 8 e-DAQ signal conditioning layers. Also includes a web interface as modern graphical user interface. And also have the ability to use the

SomatXR expansion modules, creating a powerful central data acquisition system that can also have distributed modules.



Figure 4.10: e-DAQ Processor and signal conditioning layers

4.3 Cost of experimental testing

The cost spend over the process of shaft material, machining and experimental testing is as shown below,

Sr.No.	Description	Quantity	Cost (Rs)
1	SS304 Material Bar (Diameter 40 mm)	2	2596 /-
2	Shaft Machining (Turning, Grinding, Buffing)	2	4648 /-
3	Strain Gauge	4	1890 /-
4	Experimental calibration including gauge pasting and Data Acquisition	1	16520 /-
5	Grand Total		25654 /-

Figure 4.11: Cost of experimental testing

Chapter 5

Results and Discussion

5.1 Introduction

In the development of a rotary torque sensor first the working principal is defined and further designing of shaft is carried out by considering a size and capacity of shaft. The calculation is made by selecting and considering material properties for stainless steel 304 (UNSS30400) and the analytical calculations were made. The Finite Element analysis is performed over selected torque capacity range of 100 Nm and the results are plotted. At final stage the shaft is manufactured and with practical application of strain gauge the experimentation is carried out for a capacity upto 100 Nm at the interval of 10 Nm from 0 to 100 Nm. Then all the results of analytical, FEA and experimental calibration are compared and result tables and graphs are plotted.

5.2 Material Properties and Formulas considered for Calculation

Reference Material Properties for SS304	
=Poissons ratio	0.265
E=Modulus of elasticity(N/m ²)	1.93E+11
G=Modulus of rigidity(N/m ²)	7.63E+10

Table 5.1: Material Properties

Reference Values Used for Calculation	
L=Length of shaft at gauge location(meter)	0.023
D=diameter of shaft at gauge location (meter)	0.022
R=radius of shaft at gauge location (meter)	0.011
G=Modulus of rigidity(N/m ²)	7.63E+10
J=Polar moment of inertia(m ⁴)	2.30E-08
GJ	1.75E+03
Area of Strain gauge (m ²)	6.90E-05
K=gauge factor (For metallic gauge)	2
Ev=Excitation Voltage (Volts)	12

Table 5.2: Reference values used for calculation

Formulas Used for Calculation	
Torsion Equation	$\frac{T}{J} = \frac{\tau}{R} = \frac{G\theta}{L}$
Modulus of Rigidity	$G = \frac{E}{[2(1+\mu)]}$
Polar Moment of Inertia	$J = \frac{\pi}{32} d^4$
Angle of Twist	$\theta = \frac{TL}{GJ}$
Shear Stress	$\tau = \frac{TR}{J}$
Shear Strain	$\gamma = \frac{R\theta}{L}$
Bridge Output	$e = \frac{1}{4} \cdot K \cdot Ev \cdot \epsilon$

Figure 5.1: Formulas used for Calculation

5.3 Analytical Results

Analytical Results are calculated based on values from table 5.2 and using formulas from Figure 5.1 Sample calculation for 100 Nm is,

$$\text{Shear stress} = \tau = 100 * 0.011 / 2.30E - 8 = 47.9Mpa[\text{where } J = /32 * (0.022)^4 = 2.30E - 8m^4]$$

$$\text{Shear Strain} == 0.011 * 1.31E - 3 / 0.023 = 0.000627[\text{where } \theta = 100 * 0.023 / 1.75E3 = 1.31E - 3]$$

$$\text{Bridge O/P} = 0.25 * 2 * 12 * 0.000627 * 1000 = 3.76mV[\text{Where } K = 2, Ev = 12V]$$

Torque (Nm)	Shear Stress (Mpa)	Shear Strain (ϵ)	Micro Strain ($\mu\epsilon$)	Bridge O/P (mV)
0	0	0	0	0
10	4.79	0.0000627	62.7	0.376
20	9.57	0.000125	125	0.752
30	14.4	0.000188	188	1.13
40	19.1	0.000251	251	1.50
50	23.9	0.000313	313	1.88
60	28.7	0.000376	376	2.26
70	33.5	0.000439	439	2.63
80	38.3	0.000502	502	3.01
90	43.1	0.000564	564	3.39
100	47.9	0.000627	627	3.76

Table 5.3: Analytical calculation results

5.4 Finite Element Analysis Results

Results are obtained using formulas from Figure 5.1 and FEA process by using Ansys Software for torque range from 0 Nm to 100 Nm at an interval of 10 Nm.

Torque (Nm)	Shear Stress (Mpa)	Shear Strain (ϵ)	Micro Strain ($\mu\epsilon$)	Bridge O/P (mV)
0	0	0	0	0
10	4.5041	0.00005904	59.04	0.354
20	9.0081	0.00011809	118.09	0.709
30	13.512	0.00017713	177.13	1.06
40	18.016	0.00023617	236.17	1.42
50	22.52	0.00029521	295.21	1.77
60	27.024	0.00035426	354.26	2.13
70	31.528	0.0004133	413.3	2.48
80	36.033	0.00047234	472.34	2.83
90	40.537	0.00053139	531.39	3.19
100	45.041	0.00059043	590.43	3.54

Table 5.4: FEA results

5.5 Experimental results

Experimental results are obtained directly through data acquisition system process as discussed in point 4.2.2 and strain gauge circuit output results are directly displayed in mV. During the experimental process the results obtained are with application of moment at one end of shaft which is a multiplication of load in kg into loading arm distance in meter. But converting the load into Newton by multiplying the value of gravity, the value of gravity is considered as 10 instead of 9.81 and further process is carried out and results are displayed in table 5.6

NBIP 1350 - CALIBRATION OF SS-304 SHAFT					
Load Arm Radius			0.5meter		
Sr. No.	Torque (Nm)	Load Cell Reading (Kg)	Voltage Output (mV)		
			iteration1	Iteration2	iteration3
0	0	0	0	0	0
1	10	2	0.767	0.771	0.77
2	20	4	1.153	1.159	1.162
3	30	6	1.52	1.54	1.55
4	40	8	1.9	1.88	1.9
5	50	10	2.28	2.29	2.32
6	60	12	2.64	2.66	2.67
7	70	14	3.03	3.02	3.05
8	80	16	3.38	3.4	3.39
9	90	18	3.76	3.79	3.75
10	100	20	4.13	4.15	4.15

Table 5.5: Experimental Results

5.6 Results Graphs

Graph is plotted showing the end result output comparison for all results as analytical calculation, FEA simulation results and experimental results.

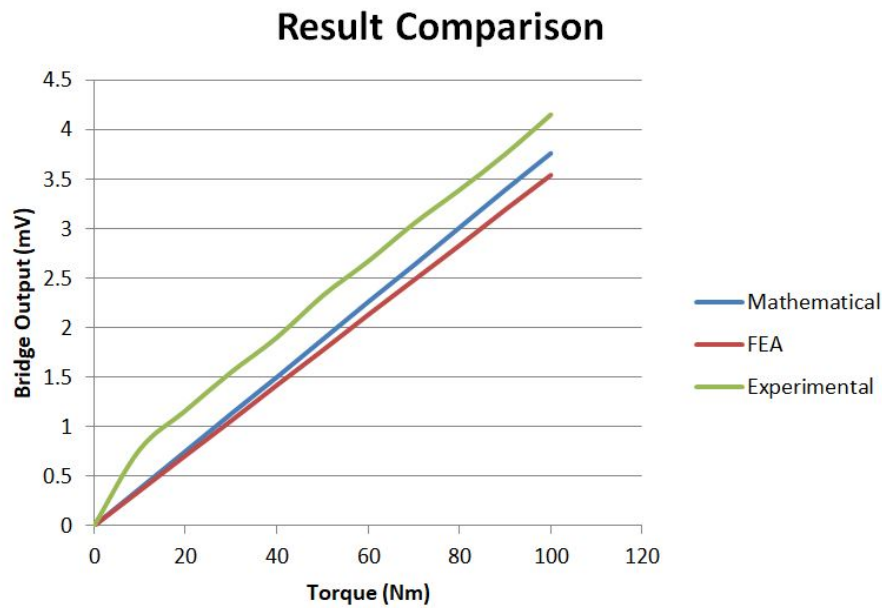


Figure 5.2: Result Comparison Graph

5.7 Discussion on Results

During the design phase it was considered that the difference in output values whether it is Analytical, FEA or Experimental should be within 20% of values in consideration. Accordingly if the comparison for 100 N.m of Analytical values with FEA values is made the difference is around 6 % (5.85). Similarly, difference in FEA values and Experimental Values is around 17% (17.23) and difference in Analytical values and Experimental Values is around 11 % (10.37).

Chapter 6

Conclusion

The design of inline rotary torque sensor by considering required performance characteristics and capacity by considering spaces for other elements of torque sensor is completed with the help of ANSYS version 2020R1. The designed core part of sensor that is the shaft on which whole sensor work is dependent is manufactured with CNC machine tool followed by the grinding process and buffing process is used at place where strain gauges are to be mounted. Then the strain gauging is done and experimental process is carried.

The results are obtained from experimental process and then compared it with mathematical calculated values and FEA values. During this whole process the assumption regarding the result co relation is that there should not be more than 20 % error in the results. So, the percentage error in the results from the mathematical calculation values with the FEA values is around 6 % (5.85). similarly difference in FEA values and experimental values is around 17 % (17.23) and difference in analytical values and experimental values is around 11 % (10.37). The results values are approximately matching with the mathematical calculation, FEA simulation values and the experimental values under the rated torque value. The differences in results are may be due to the experimental temperature condition during experimentation, Strain gauging errors while pasting, manual errors happened during the process of experimentation also some material property fluctuations and assumptions made during the whole process Hence the core part is completed with design manufacturing and experimentation.

- Future Work:-

The proposed design of sensor including all the required elements to make the sensor as a complete unit is completed. Also manufacturing of the core part that is the shaft and experimentation is completed to obtain desired results. But the future work for remaining part of the sensor is developing the electronics of the sensor that is the slip ring and brushes assembly can be completed in near future so that a whole sensor can be utilized as a production ready unit.

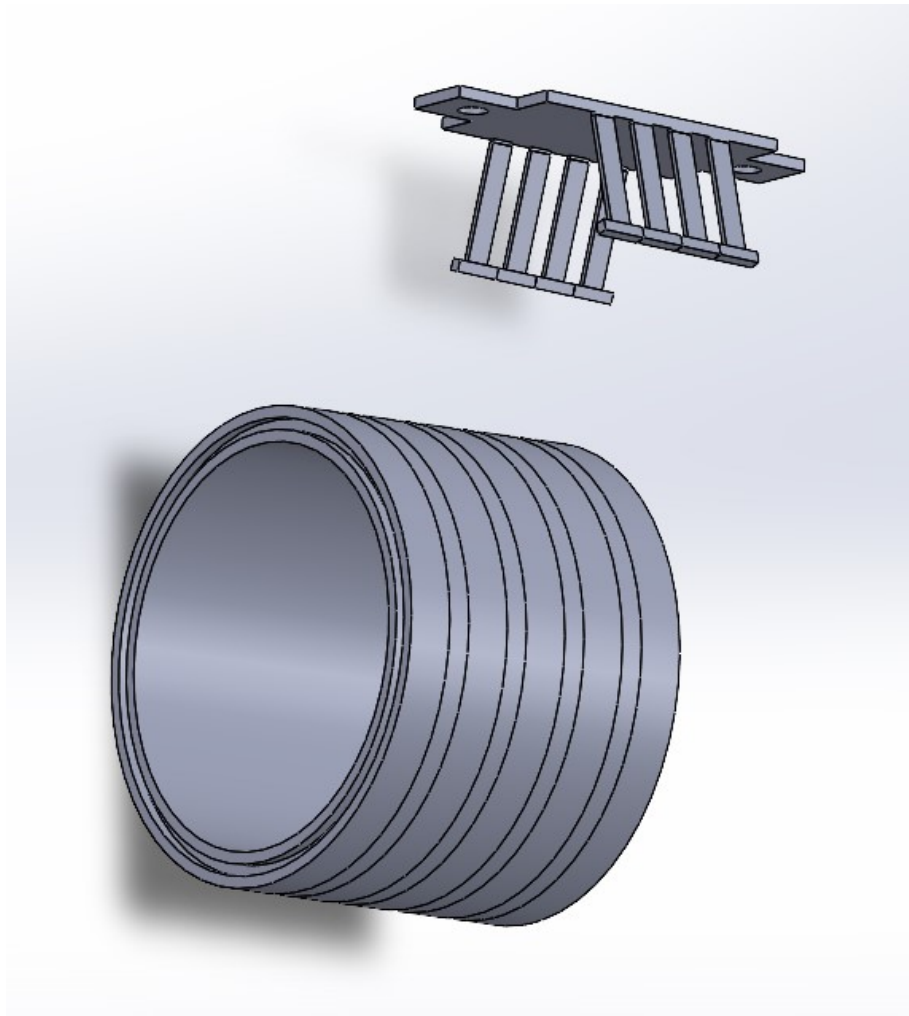


Figure 6.1: Proposed design of Slip ring and Brushes

LIST OF PUBLICATIONS ON PRESENT WORK

- [1] S. S. Powar, Dr. M. B. Mandale, “Design and Development of a Rotary Torque Sensor ”International conference on Recent Advances in Engineering and Technology (RIT-RAIET 2021)
- [2] S. S. Powar, A. S. Koli, Dr. M. B. Mandale, “Design and Development of a Rotary Torque Sensor ”International Journal on Advanced Science Engineering and Information Technology.(Under review)

REFERENCES

REFERENCES

- [1] Westbrook and Turner, 1994. "A strain gauge based system for measuring dynamic loading on a rotating shaft", *International Journal of Mechanics*, vol. 5(1), pp. 19-26.
- [2] Kovacich, Ani. K and Sanjiv. G. 2002. Design Studies and Testing of Torque Transducer. *Indian Journal of Pure and Applied Physics* Vol. 49, October 2011, pp.653-656.
- [3] Fulmek, Madni and Susumu Tachi 2004 Torque Sensors for Robot Joint Control [researchgate.net/publication/221787482](https://www.researchgate.net/publication/221787482)
- [4] Hamza Khan, Claudio Semini, and K. Koichi, 2017. "Development of New Magnetostrictive Torque Sensor for Automobile Power Train System," *Hitachi Cable*, No.26/ PP.41-44, 2017.
- [5] Zhang Jiaming, Gong Chen and K. Yamakawa, 2015. "Improvement of the angular dependent noise in a magnetostriction type torque sensor," *International Journal of Automotive Engineers*, vol. 2, no. 3, pp.75–80, 2015.
- [6] Dieter Doerrie, Paul Schwerdt, Wenrui Wang and Hao Sun, 2014. Design and Application of Strain Brushless Torque Sensor *International Conference on Advanced Manufacturing and Industrial Application (ICAMIA 2014)*
- [7] M. H. Muftah, S.M. Haris and Franz Haas, Reinhard Marik, 2010. contactless torque sensor 6th *International Conference on Informatics in Control, Automation and Robotics ICINCO 2010*
- [8] Zhigang chu, Hongyu shu, Chongdu Choc, 2020. Design of a New Non-contact Torque Sensor for Rotating Stepped Shaft by Monitoring Magnetic Field *Applied Mechanics and Materials* Vols. 44-47 (2020) pp 547-551
- [9] H. Defu, Min Li, Yu Xiang Sun, 2015. "Design of the strain torque sensor," *Ship Engineering*, vol. 194, pp. 96-99, April 2015.

[10] Hong Liu, Yiwei Liu, L. Zeming, G. Shiqing, "Study on design principle of strain torque sensor," *Machinery Design & Manufacture*, vol. 248, pp. 13-15, October 2014.

[11] Dae-Han Hong, Jinung An "Miniature force-torque sensor using semiconductor strain gage sensor frame design and analysis for development" 10.1109/URAI.2012.6463101 IEEE November 2012

[12] Vischer and Khatib, Yu-Xiang Sun 1995 "Design of a novel six-axis force/torque sensor based on strain gauges by finite element method," 10.1109/WCICA.1995.7053277 IEEE.

[13] Shinoura, Yiwei Liu, 2003. "Design of a novel six-axis force/torque sensor based on strain gauges by finite element method," 10.1109/WCICA.2003.7053277 IEEE.

[14] Hubert Gattringer, Andreas Muller, and Hao Wang, 2021. "An Experimental-Numerical Combined Method to Determine the True Constitutive Relation of Tensile Specimens after Necking," Volume 2021 |Article ID 6015752 | <https://doi.org/10.1155/2021/6015752>.
Hindavi advances in material science and technology

[15] Hirose and Yoneda, Jin weon kim 1990, "Determination of true stress-strain curve of type 304 and 316 stainless steels using a typical tensile test and finite element analysis," <https://doi.org/10.1016/j.net.1990.07.014>. Nuclear Engineering and Technology.

[16] Takahashi, Mariapaola D'Imperio, Ferdinando Cannella, Darwin G. Caldwell, Towards Scalable Strain Gauge-Based Joint Torque Sensors www.mdpi.com/journal/sensors Sensors 2003, 17, 1905; doi:10.3390/s17081905

[17] HBM Products Catalog, Hottinger Baldwin Messtechnik GmbH, Germany, 2020.

SYNOPSIS

Approved Copy of Synopsis
Page..01..03

K.E. Society's
Rajarambapu Institute of Technology, Rajaramnagar
(An Autonomous Institute, affiliated to Shivaji University, Kolhapur)

SYNOPSIS OF M. TECH DISSERTATION

1. **Name of college:** Rajarambapu Institute of Technology, Rajaramnagar
2. **Name of course :** M.Tech Mechanical Design Engineering.
3. **Name of student :** Suraj Shankar Powar (PRN-1921005)
4. **Date of registration :** August 2020
5. **Name of the Guide :** Dr. M. B. Mandale
6. **Proposed Title :** Design and development of a Rotary Torque Sensor.
7. **Sponsored by :** TRILON Technology, Pune, Maharashtra.
8. **Company Supervisor :** Mr. Aniket Koli

9. **Synopsis of proposed work:**

9.1) **Relevance:-**

Torque measurement need is increased as more and more mechanical product capacity is developed. The measurement of torque is essentially required to the control part of power transmission system for the improvement of machine efficiency. Therefore, the sensing and measurement of torque in an accurate, reliable and inexpensive manner is needed. So a new torque sensor concept based on a highly reliable sensing principle is needed to be developed. The basic idea is the transformation of the shaft twist under torque load into a translational input of sensing element measured and displayed by measuring device.

This new sensor concept is very robust and self compensating for all kinds of relative positioning tolerances ranging from temperature change to external forces.

9.2) Literature Review:

Torque measurement on rotating shafts leads to a specific design requirement. The torque information has to be transmitted from the rotating shaft to the static readout environment. The technical solution is to pick up the torque information on the rotating shaft and transmit it to a stationary receiver either through electric, magnetic or electromagnetic field.

Mechanical Domain:

[1] Jacobsen et al. The twist of a steel shaft under load is transformed to an axial displacement in . This effect and the core part of the torque sensor. The applied torque causes a shaft twist that is induced into a specially designed sleeve. This part, for instance made of aluminium, is perfectly attached to the shaft at two cylindrical faces with a constant distance. The connections of the middle part to the outside parts represent thin rods that translate the twist into a translational movement along the shaft rotation axis. Possible manufacturing processes are chipping technologies (turning and milling), powder injection moulding or welded composite from punched parts depending on the production volume.

Electrical Domain:

[2] Franz Hass et al. Electrical measurement is essentially associated with strain gauges, capacitive, and piezoelectric sensing. Strain gauge operation is based on variations in electrical resistance with strain. When force is applied, strain changes the electrical resistance of gauges proportionally to the load. Silicon semiconductor strain gauges are often used due to high sensitivity. Strain in silicon causes its bulk resistance to change, producing a signal 75 times stronger than conventional foil gauges where resistance changes are only due to dimensional changes in the resistor. Despite such benefits of strain gauges as high linearity, about 0.03%-2.5% of full scale (FS), high resolution of 1-3 mV/V, their maximum allowable strain is close to their breaking point. To guarantee overload protection of transducers, mechanical stops limiting deflections of flexures are necessary. Very stiff sensors may only deflect a few ten-thousandths of a millimeter. Production of limit stops with such small clearances is very difficult. Strain-gauge-based torque/force sensors are greatly subjected to radial and other force components. Semiconductor and foil gauges require elaborate process for attachment by a specialist. Another shortcoming of these sensors is their high sensitivity to electrical noise and temperature.

[3] Westbrook & Turner et al. Piezoelectric torque sensors are similar in operation to strain gauges and based on the phenomenon, in which a crystal becomes electrically charged under the action of mechanical stress. High stiffness and strength enable sensors to be directly inserted into the torsion member.

[4] Kovacich Fulmek et al. An example of the piezoelectric effect is the invention where authors exploited changes in the resonant frequency of the piezoelectric element as a measure of the strain, to which the torsion member is subjected. Extremely high accuracy (0.03% of FS) and high signal output are their main advantages. Drawbacks restricting their application are high cost and nonlinear output. Many torque transducers are based on measuring the relative angle between the two ends of the torsion bar. This principle was realized in the differential capacitive sensor for measurement of the relative angle. The transducer is noncontact, robust, and compact. Two rotatable electrodes are placed between two sensor plates. The relative angle between the two rotors and the absolute position of the rotor blades are calculated from measurement of capacitive coupling between different transmitting stator segments and a single receiving electrode. Its drawback is high sensitivity to radial displacement and high cost.

[5] Madni et al. The relationship between the capacitor capacity and permittivity of the dielectric material between the capacitor plates also was used in patent. In this invention, the apertured metal cage shielding a dielectric rotor is placed between capacitor plate rings fixed on opposite sides of a torsion bar. The relative rotation of the apertured conductive plates and the dielectric rotor changes the overall differential capacitance of the system in proportion to torque.

Electromagnetic Domain:

[6] K. Yoshida et al. In electric power steering system torque sensor plays an important role for detecting the drivers steering operation as steering torque data and sending this information to the electronic control unit as a signal. Conventionally printed circuit boards with general purpose surface mounted devices have been used to receive and amplify the torque signal detected by the pair of torque sensor coils. Recently the energy saving benefits of electric power steering has been receiving much attention and the number of cars equipped with electric power steering system has been increasing. On a custom IC for a electric power steering torque sensor that enable torque sensor printed circuit boards to be smaller have fewer electronics parts and be cheaper.

[7] Vischer & Khatib et al. Faraday's law is used linear variable differential transformers (LVDT) in the torque sensor. The main advantage of LVDT is their high degree of robustness, remarkable resolution of about $0.1\mu\text{m}$, good accuracy (0.01-0.3%), and easy installation and calibration. High reliability is derived from their operation principle based on magnetic transfer eliminating physical contact across the sensing element. The strong relationship between core position and output voltage of secondary coils yields excellent resolution. Inductive sensors suffer from reduction in signal at very low frequencies, and they are affected by electromagnetic noise. The smallest LVDT made by the Lucas Schaevitz in XS-B series weighs only 4.36 g and has an outer diameter of 4.77 mm, but its length of 22.4 mm complicates compact overall dimensions of the torque transducer.

[8] Ishino Shinoura et al. The effect, in which stress applied to the material causes a change in its magnetization, is known as the Villari effect or magnetostriction phenomena. Magnetostrictive torque sensors consist of rotational shaft, having a magnetostrictive metal layer of a chevron configuration formed on the shaft, an exciting coil, and a pickup coil for detecting the magnetic property change of the magnetostrictive layer. When AC current is applied to the exciting core, the magnetostrictive layer is excited. Torque applied to the magnetostrictive element generates stress. Permeability is changed by the Villari effect, and inductive output is generated in the pickup coil with torsional load. Advantages of the sensor are nonphysical contact between the shaft and housing, and high torsional stiffness. Drawbacks are complicated manufacturing, bulky heavy structure, need for a robust magnetic shield, and insufficient performance (linearity of 3-5% FS, hysteresis of 2-3%, resolution of 10 mV/V)

Optical Domain:

[9] Dzmitry Tsetserukou et al. A light source, photosensor, and solid object modifying the amount of light incident on the optical detector are necessary to measure displacement between unmovable and flexible parts of the optical sensor. Photosensors have such drawbacks as nonlinearity and temperature sensitivity, but they are considerably more reliable, cheap, and simplified in design than other sensors. A displacement is detected by interrupting light between source and detector, changing the intensity of reflected light, or the relative movement of source and detector.

[10] Hirose & Yoneda have significantly contributed to research on the optical force/torque sensors. They proposed using a split photosensor to detect displacement of the light source

(LED) caused by applied force in two directions. a force loaded adapter plate, a load cell (elastic element), a photodetector, a LED, an installation adapter plate. When force is applied to the plate, elastic solid body deflects LED light incident on photosensor. Thus, magnitude of the photodetector output responds on exerting force/moment. In cooperation with the Minebea Co., OPFT series of 6-axis optical force/torque sensors were manufactured. Compared to conventional strain-gauge-based transducers, they are more compact, lightweight, and cheap, but they have complicated calibration due to nonlinear output, require application of DSP for real-time computation of measured force, and have an average accuracy of 5% FS. At Nara Institute of Science and Technology, a 6-axis optical force/torque sensor was developed for fMRI application

[11] Takahashi et al. The sensor was made from acrylic resin to eliminate any metal sensor components that generate fMRI signal noise. The layout of the transducer is shown in Fig. 3. The elastic frame has a Y-topology with S-shaped beams to enable 6-DOF displacement of the sensing face. Force exerted by users deflects the elastic frame, altering the intensity of light falling on optical fiber. The sensor provides accuracy of 2.65% for measurement of moment MZ. The transducer is complicated and intended only for narrow applications. The transducer is shown in Fig. 3. The elastic frame has a Y-topology with S-shaped beams to enable 6-DOF displacement of the sensing face. Force exerted by users deflects the elastic frame, altering the intensity of light falling on optical fiber. The sensor provides accuracy of 2.65% for measurement of moment MZ. The transducer is complicated and intended only for narrow applications.

Research Gap:

Through literature review, it has been observed that there is much amount of work is done on torque sensor by different working principles but still with requirement of different application base and so much autonomy work, development of torque sensor for particular or unique application there is scope of developing a torque sensor considering different parameter improvements with respective working conditions at an affordable cost and manufacturing it.

9.3) Problem statement:

Modern era always looks to modify and upgrade technology, cost plays an important role for accessing the technology, therefore designing and developing a rotary torque sensor by improving the performance characteristics in accordance to the relative positioning changes and to work with respective working conditions ranging from temperature change to external forces more efficiently and manufacturing it at an affordable cost completely. There is need to study those aspects of developing the sensor with improvisation in the performance.

9.4) Objectives:

1. To study various working principles and operating methods of different types of torque sensors.
2. Determine methodology and select best suitable working principle by considering performance characteristics such as working environment, nonlinearity, hysteresis, rotational speed and rated output.
3. Prepare conceptual design and develop it according to specified performance characteristics and perform its finite element analysis.
4. To check the manufacturing feasibility with best suitable manufacturing technique at controlled cost for accurate torque value measurement.

9.5) Proposed work:

Phase-wise Plan,

Phase 1: Literature survey

This phase consists carrying out literature survey by referring reputed journals from reputed publishers like Elsevier, Science Direct, ASME, IEEE, Taylor and Francis and previously published master and Doctoral thesis in the area of Torque sensor application. Also, the work related to different measurement principle and methodology will be studied. This will help to gain theoretical background regarding project.

Phase 2: Selection of working Principle

In this phase working principle is selected by studying different ways of working methodology such as mechanical, electrical, electromagnetic and optical. One of them is selected to do further development considering required parameters and working condition.

Phase 3: Design and optimization

In this phase Torque Sensor will be designed and developed according to selected methodology to have the required output performance under predetermined working condition.

Phase 4: Feasibility for manufacturing

In this phase the feasibility for manufacturing of the sensor will be checked as per design data with best suitable manufacturing technique by taking care of small and important parts of sensor with accurate and precise dimensions.

Phase 5: Testing and validation of results

Results of experimental testing in actual working condition and validation of results by calibrating it with suitable methods of torque calibration in accordance with ISO 9000 and IATF 16949.

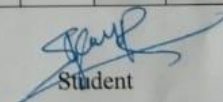
9.6) Expected outcome: -

The rotary torque sensor designed and developed after studying different principles and methodology with respect to required performance characteristics and working environment conditions using simulation software and later manufactured it to have accurate and precise measurement of torque quantity for the application and continuous monitoring of torque data for the improvement of efficiency of plant.

9.7) Plan of proposed work:

Sr.No.	Activity/ Month	Aug	Sept	Oct	Nov	Dec	Jan	Feb	Mar	Apr	May
1	Literature survey	█	█	█							
2	Study and section of methodology			█	█	█					
3	Concept design					█	█				
4	Design and optimization							█			
5	FEA analysis						█	█			
6	Manufacturing feasibility								█	█	
7	testing and validation of results								█	█	
8	Report writing										

9.8) Expected date of completion of work: -May 2021.

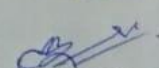

Student


(Suraj Shankar Power)



Company Supervisor
(Mr. Aniket Koli)




Guide & Head of Program
(Dr. M. B. Mandale)

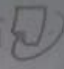


Head of Department
(Dr. S. K. Patil)

9.9 References:-

- (1) Hashimoto, M.; Horiuchi, M. & Ninomiya, T. (2001). Performance of gain-turned harmonic drive torque sensor under load and speed conditions. IEEE/ASME Transaction on Mechatronics, Vol. 6, No. 2, (June 2001) 155-160, ISSN 1083-4435
- (2) Multi-Axis Force/Torque Sensor, ATI Industrial Automation, [Online], Available: <http://www.ati-ia.com>.
- [3] Frank Umbach, Heinrich Acker, Johannes von Kluge and Werner Langheinrich: Mechatronics Vol. 12 (2002), p. 1023-1033
- (4) Shinoura, O. (2003). Torque sensor and manufacturing method of the same. U.S. Patent 6 574 853, June 2003.
- (5) Passenger Car Steering Systems – Preparation for the Technology of Tomorrow (26-27/04/2005 in Essen) Introduction presentation by Dr.-Ing. Alois SEEWALD
- (6) "Position sensor, design in particular for detecting a steering column torsion", US patent publication number #2004-0011138
- (7) W. Ijiri, T. Daido, M. Sugimoto, S. Hirakushi: Koyo Engineering Journal, 134 (1988) 48.2)
M. Taniguchi, H. Nagano: Koyo Engineering Journal, 137(1990) 68.
- (8) Angleviel, D., Frachon, D., and Masson, G., 2006. Development of a Contactless Hall effect torque sensor for Electric Power Steering. MMT S.A.
- (9) Jacobsen, A.M., Electrical Dynamometer. US Patent Application Serial No. 561,467. Los Angeles.
- (10) Product documentation of the sensor interface. Graz..
Seiffert, U., Rainer G., Virtuelle Produktentstehung für Fahrzeug und Antrieb im Kfz. pp 7-29. Vieweg+Teubner Verlag. Wiesbaden.
- (11) Towards scalable strain gauge based joint torque sensors, MDPI. Hamza Khan, Maria Paola Dimperio, Darwin G Caldwell, Claudio Semini.
- (12) An improved strain gauge based dynamic torque measurement method, Journal of circuits systems and signal processing. M. Hilal Muftah, S. Mohamed Haris, K. Petroczki and E. Awad Khidir

PLAGIARISM CHECK REPORT

turnitin 

Suraj Project Report updated 24(1).doc
Sep 23, 2021
9209 words / 46173 characters

Suraj Powar
design and development of a rotary torque sensor).doc

Sources Overview

8%
OVERALL SIMILARITY

Source	Similarity
1 www.intechopen.com INTERNET	2%
2 www.naun.org INTERNET	2%
3 Swansea Metropolitan University on 2016-11-29 SUBMITTED WORKS	<1%
4 Swansea Metropolitan University on 2016-04-19 SUBMITTED WORKS	<1%
5 tachilab.org INTERNET	<1%
6 Edinburgh College (New) on 2014-11-07 SUBMITTED WORKS	<1%
7 University of Moratuwa on 2020-10-21 SUBMITTED WORKS	<1%
8 University of Northumbria at Newcastle on 2014-08-14 SUBMITTED WORKS	<1%
9 Sim University on 2021-05-09 SUBMITTED WORKS	<1%
10 Isik University on 2017-11-09 SUBMITTED WORKS	<1%
11 International Islamic University Malaysia on 2018-04-16 SUBMITTED WORKS	<1%
12 Edinburgh College (New) on 2015-10-02 SUBMITTED WORKS	<1%
13 Ran Shu, Zhigang Chu, Hongyu Shu. 'A Lever-Type Method of Strain Exposure for Disk F-Shaped Torque Sensor Design', Sensors, 2020 CROSSREF	<1%

Excluded search repositories:

- None

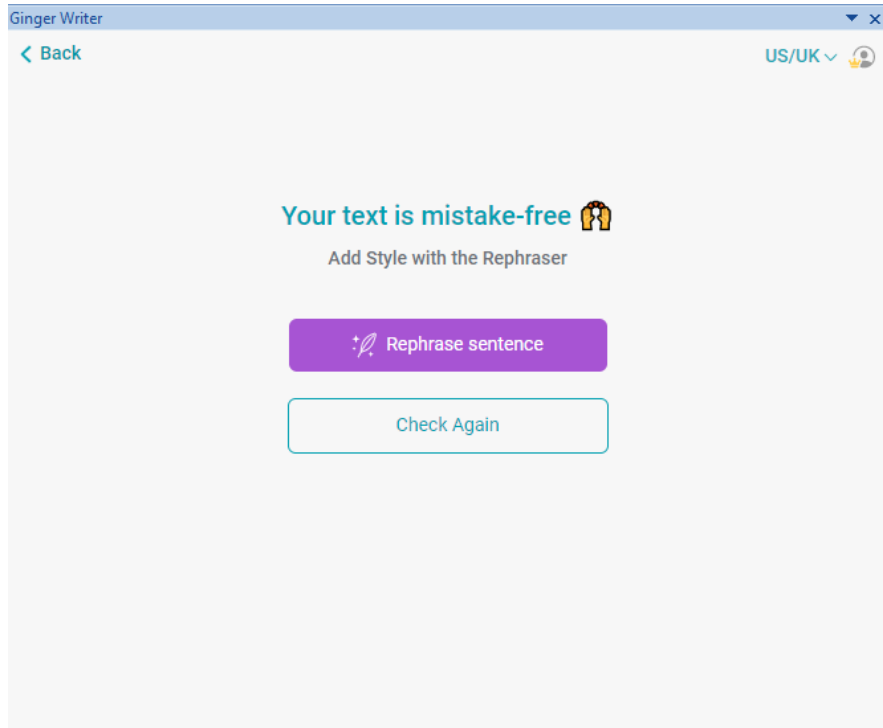
Excluded from Similarity Report:

- Bibliography
- Quotes
- Citations

*Checked - Gondil VB
23/09/2021 - Gondil VB*

1 of 52 9/23/2021, 1:14 PM

GRAMMER CHECK REPORT USING GINGER



JOURNAL PAPER

International Journal on Advanced Science, Engineering and Information Technology

[HOME](#) [ABOUT](#) [USER HOME](#) [SEARCH](#) [CURRENT](#) [ARCHIVES](#) [ANNOUNCEMENTS](#)

[Home](#) > [User](#) > [Author](#) > [Active Submissions](#)

Active Submissions

ACTIVE [ARCHIVE](#)

<u>ID</u>	<u>MM-DD SUBMIT</u>	<u>SEC</u>	<u>AUTHORS</u>	<u>TITLE</u>	<u>STATUS</u>
16326	09-22	ART	power	DESIGN AND DEVELOPMENT OF A ROTARY TORQUE SENSOR	IN REVIEW

1 - 1 of 1 Items

CONFERENCE PAPER



Kasegaon Education Society's
Rajarambapu Institute of Technology, Rajaramnagar
Islampur, Dist – Sangli (MH), India (PIN : 415414)



(An Autonomous Institute, affiliated to Shivaji University, Kolhapur)

National Conference on
"Recent Advances in Engineering and Technology"

◀ ○ Certificate ○ ▶

This Certificate is awarded to Mr./Ms. S.S. Powar

of Rajarambapu Institute of Technology, Rajaramnagar presenting paper entitled
Design and Development of a Rotary Torque Sensor in the Track Mechanical - Design
at National Conference on "Recent Advances in Engineering and Technology" (RIT - RAIET) held on
6th August 2021.

Dr. M. S. Kumbhar
Organizing Secretary

Dr. S. S. Gawade
Co-Convener

Dr. L. M. Jugulkar
Convener

Dr. S. K. Patil
Dean, Academics

Dr. Mrs. S. S. Kulkarni
Director

CV

CURRICULUM VITAE

SURAJ SHANKAR POWAR

Address: Powar Jadhav lane near Biroba Temple,
Shiroli Pulachi Pin-416122
Email: surajpowar0941@gmail.com.
Mobile: +91-9975373379/+91-9405182181



Career Objective:

To make optimum utilization of my knowledge and skills, utilize opportunities effectively for professional growth and to contribute in best possible way for the betterment of the organization and self.

Academic Qualification:

Examination	College/School	Board/University	Percentage	Year of Passing
Masters in Mechanical Design	Rajarambapu Institute of Technology, Islampur	AUTONOMOUS (Shivaji University)	First Year 7.92 CPI	Pursuing (2019-21)
Bachelor in Mechanical Engg.	Sanjay Ghodawat Group Of Institutions, Atigre.	Shivaji University, Kolhapur	62%	2019
Diploma in Mechanical Engg.	Karmyogi Polytechnic Collage, Shelve Pandharpur.	Maharashtra State Board Of Tech. Education	82.94%	2016
SSC	Madhyamic Vidyalaya , Kurlap.	Maharashtra State Board, Kolhapur division	76.80%	2013

Software Proficiency:

- HYPERWORKS
- ANSYS
- SOLIDWORKS
- AUTO CAD

Key Skills:

- Quick Learner
- Good Team Player and Flexible at work.
- Work under pressure with Positive Attitude.
- Good People Handling and Convincing skills.
- Hard Working Ability, hard working with smart way.

Academic Project:**[1] Diploma Project: Manufacturing a model of Spiral Binding Machine.**

Team Size	4 members
Project Duration	1 Year
Project Synopsis	The purpose of this project was to Reduce The Fatigue Of Humans For Spiral Binding And To Make A Portable Device To Carry Punching And Binding Operations At One Place.
Key Role	Worked as team leader.

[2] UG Project: Designed & Fabricated a stair climbing wheelchair for disabled peoples.

Team Size	5 members
Project Duration	1 Year
Project Synopsis	The purpose of this project was to design, fabricate and validate a stair climbing wheelchair for the disabled peoples in our society.
Key Role	Team leader as well as manufacturing head.
Project Achievement	Innovative idea appreciation.

[3] PG Project: Design and development of a rotary torque sensor.

Team Size	1 (self)
Project Duration	1 Year
Sponsored by	Trilon Technology Pune
Project Synopsis	To design and develop a rotary torque transducer based on electrical principle to have precise measurement of torque value.

Achievements and Extra Co-curricular Activities:

- Got "Innovative Idea" appreciation for project.
- Attended Business Idea workshop held by Gov. of Maharashtra in Pandharpur.
- Participated in 2 days program on CNC machine coding and overview.
- One month Industrial training at Kaneri Enterprises Shirolī-Kolhapur.
- Five week virtual internship program on Role of Smart and Composite materials in structural design.

Personal Details:

- Date of Birth: -6th July 1997.
- Father's Name: -Shri. Shankar G. Powar
- Marital Status : -Single
- Gender : -Male
- Hobbies : - Sketching, Travelling, Reading, Learning new design skills
- Languages Known: - Marathi, Hindi, English.
- Permanent Address : - Powar-Jadhav lane, Near Biroba Temple, Shirolī Pulachi Taluka:-Hatkanangale District:-Kolhapur. Pin:- 416122

Declaration:

I hereby declare that information furnished above is true to the best of my knowledge.

- Date:
- Place:

SURAJ S. POWAR